

Fabrication, Characterization and Modelling of Piezoelectric PVDF-TrFE polymer as a Force
Sensor Using Spin Coating Method

Saman Namvarrechi

A Thesis
In the Department
of
Mechanical, Industrial and Aerospace Engineering

Presented in Partial Fulfillment of the Requirements
For the Degree of Master of Applied Science at
Concordia University
Montreal, Quebec, Canada

January 2021

© Saman Namvarrechi, January 2021

CONCORDIA UNIVERSITY

SCHOOL OF GRADUATE STUDIES

This is to certify that this thesis is prepared

By: Saman Namvarrechi

Entitled: Fabrication, Characterization and Modelling of Piezoelectric PVDF-TrFE
Polymer as a Force Sensor Using Spin Coating Method

and submitted in partial fulfillment of the requirements for the degree of

Master of Applied Science (Mechanical Engineering)

complies with the regulations of the University and meets the accepted standards with respect to originality and quality.

Signed by the final examining committee:

_____ Chair
Dr. Mojtaba Kheiri

_____ External Examiner
Dr. Amin Hammad

_____ Examiner
Dr. Mojtaba Kheiri

_____ Thesis Supervisor
Dr. Javad Dargahi and Dr. Mojtaba Kahrizi

Approved by

Dr. Narayanswamy R Sivakumar

January 22, 2021

Dr. Mourad Debbabi , Dean
Gina Cody School of Engineering & Computer Science

Abstract

Fabrication, Characterization and Modelling of Piezoelectric PVDF-TrFE Polymer as a Force Sensor Using Spin Coating Method

**Saman Namvarrechi, MAsc.
Concordia University, 2021**

Since last decades, needs of new valuable material and reliable sensing technologies were among the researchers focus for different industry's application. Piezoelectric Polyvinylidene Fluoride (PVDF) polymer and its copolymer, Trifluoroethylene (TrFE), are one of these materials that can be a strong candidate for new transducers and sensors due to its electromechanical properties for force/pressure sensing in different industries such as biomedical device companies. Since PVDF is Biocompatible, a thin film of it can be integrated with biomedical devices using adhesive materials. However, it is not advisable for biomedical devices/tools to use those materials due to potential toxicity of gluing different objects inside human body. An example of such devices is laparoscopic tools used in Minimally Invasive Surgery (MIS), where PVDF film is deployed at the tip of an endoscopic grasper for force and softness sensing. To avoid toxicity problem, it is possible to deposit PVDF film directly on a potential device using a spin coating approach and fabricate it from scratch. However, it has its own challenges.

In this research, PVDF-TrFE polymer is deposited via spin coating method and treated with various post-deposition processes to investigate its piezoelectricity and amount of electroactive β phase. These processes include different post thermal annealing, the effect of spin coating speed, different layer of deposition and presence of additional hydrate salt. Using FTIR spectroscopy and SEM images, the amount of the β phase and porosity of each sample is determined. In addition, the optimum experimental study is established by considering every aspect of the fabrication process.

Finally, sample sensors are tested, their output voltage signal are verified, and the results are compared to the Comsol simulation software. This study clearly shows the effective way of deposition and fabrication of a tactile PVDF-TrFE based sensor and an enhancement methodology to have a higher β phase, piezoelectric constant and higher output voltage in order to have a better force/pressure sensitivity for different applications such as MIS's end effector.

Acknowledgments

First of all, I would like to express my intense gratitude to my supervisors, Dr. Javad Dargahi and Dr. Mojtaba Kahrizi, for the continuous support of my research and their critical supervision. Their guidance helped me in all the time of research and writing this thesis.

Moreover, I would like to take the opportunity to thank all of my lab-mates: Armin Agharazy Dormany, Amir Hooshier, Naghmeh Bandari, Amir Molaei, Mohammad Jolaei, Masoud Razban, Majid Roshanfar, Sevin Samadi, Hamid Reza Nourani, Amir Sayadi, Nima Amooye, Pedram Fekri and Ali Akhalaf for their motivation, support and valuable advice. During my masters, not only have they always answered my questions with patience and helped me through the difficulties of the research, but also for being a friend, giver, honest and real to me.

Warm and heartfelt gratitude also goes to my friends: Nikta Tabesh, Hamed Khanzadeh, Sam Bahman, Golnoosh Karimipourfar, Mikail Arani, Parsa Bandamiri, Nargess Amini, Mohammadreza Chartab, Majid Rahimi and many others who endlessly supported me and persistently were by my side in all the stages of my master's study.

Last but not least, I must express my profound gratitude and special sincere to my Parents, brother, sisters and my uncle for providing me with unfailing support and invaluable care not only during my years of study but also throughout my whole life. No words can express my love to my family and this accomplishment would not have been possible without them.

Many thanks to all of you!

Saman Namvarrechi

List of Publications and Conference Contributions

- [1] Namvarrechi, Saman, Armin Agharazy Dormeny, Javad Dargahi, and Mojtaba Kahrizi. "Fabrication and Characterization of Piezoelectric PVDF-TrFE Sensor Fabricated Using Spin Coating Method for Biomedical Device Applications." In *2020 International Conference on Biomedical Innovations and Applications (BIA)*, pp. 33-36. IEEE, 2020.

*This thesis is dedicated to my family for their
endless love, support and assistance*

TABLE OF CONTENTS

LIST OF FIGURES	x
LIST OF TABLES	xii
LIST OF ACRONYMS	xiii
LIST OF SYMBOLS	xiv
Introduction	1
1.1 Introduction	1
1.2 Piezoelectric Effect and Polymers	1
1.3 Pyroelectricity	3
1.4 Fabrication Processes and Deposition Methods	5
1.5 Objective of the research	5
1.6 Organization of the thesis	6
Literature Review: Piezoelectricity and Piezoelectric Polymers, Characteristics and synthesis Methods	8
2.1 Piezoelectricity	8
2.1.1 Direct and Converse Piezoelectric Effects.....	8
2.2 Piezoelectric Materials	11
2.2.1 Ceramics	13
2.2.1.1 Quartz	13
2.2.1.2 Barium Titanate (BaTiO ₃)	13
2.2.1.3 PZT Ceramics	13
2.2.2 Polymers	14
2.2.2.1 PVDF and Its Blends with TrFE.....	14
2.3 Fabrication Methods of β-phase PVDF	18
2.3.1 PVDF Copolymers.....	19
2.3.2 Solvent Casting	20
2.3.3 Effect of Thermal Annealing	21
Instrumental and Experimental Procedure	22
3.1 Fabrication Process and Experimental Procedure	22
3.2 Materials Preparation	24
3.2.1 Polyvinylidene Fluoride-Trifluoroethylene (PVDF-TrFE).....	24
3.2.2 N,N-Dimethylformamide (DMF).....	25
3.2.3 Acetone	26
3.2.4 Mg(NO ₃) ₂ ·6H ₂ O	26
3.3. Laboratory Sections, Devices and Procedures	27
3.3.1 Cleanroom and Spin-Coating Device.....	27
3.3.2 Evaporating Machine	28
3.3.3 Wet Lab.....	29
3.3.4 FTIR Device.....	30
3.3.5 SEM	31
3.3.6 Confocal Microscopy	32
PVDF-TrFE Fabrication Process	34
4.1 Solution Preparation	34

4.2 Substrate Preparation	34
4.3 Spin Coating	35
4.4 Post Thermal Annealing.....	35
Characterization of PVDF-TrFE Piezoelectric Polymer	38
5.1 Effect of Post Thermal Annealing	38
5.2 Thickness Test	41
5.3 FTIR Characterization.....	42
5.4 Effect of Hydrate Salt	45
Experimental Testing, Voltage Results and Computer Simulation	47
6.1 Experimental Setup	47
6.2 Applied Force and Output Voltage	49
6.2.1 Results and Analysis	52
6.3 Piezoelectric Coefficient Calculation.....	54
6.4 Computer Simulation with COMSOL	56
6.4.1 Device Modelling and Simulation Setup	56
6.4.2 Force Distribution and Stress Results	58
6.4.3 Simulation Results and Output Voltages	59
6.4.4 Analysis and Comparison	60
Conclusion and Future Works	62
7.1 Conclusion and Contributions	62
7.2 Future Works	64
7.2.1 Poling	64
7.2.2 Pyroelectricity Test	64
References	65

LIST OF FIGURES

Figure 1. 1 (adopted from Azo Materials [2]) Direct and converse effect in piezoelectric materials. (a) When a voltage is applied across a poled piezoelectric device, the material expands in the direction of the field and contracts perpendicular to the direction of the field. (b) When a force is applied to the piezoelectric, an electric field is generated. 2

Figure 1. 2 (adopted from Lang [13]) “If a pyroelectric crystal with an intrinsic dipole moment (top) is fashioned into a circuit with electrodes attached on each surface (middle), an increase in temperature prompts the spontaneous polarization to decrease as the dipole moments, on average, diminish in magnitude. The horizontal tilting of the dipoles, pictured at the bottom, signifies the effect. Current flows to compensate for the change inbound charge that accumulates on the crystal edges.” 4

Figure 2. 1 (adopted from Tandon [23]) Direct and converse piezoelectricity. 9

Figure 2. 2 (adopted from Tichy [24]) Applications of direct and converse piezoelectricity. 10

Figure 2. 3 (Adopted from [25]) Axis definition for the piezoelectric coefficients in different directions. 11

Figure 2. 4 (Adopted from Kim [26]) “The classification of insulator materials according to the physical properties.” 12

Figure 2. 5 (Adopted from Zhu [40]) Chain structures of α , β , and γ phases of PVDF. 16

Figure 2. 6 (Adopted from Lovinger [42]) Transformation between the crystalline phases of PVDF. 17

Figure 2.7 (Adopted from Yu [60]) “Phase transformation in PVDF polymer due to the electrical polling, cold drawing, and annealing under high pressure.” 19

Figure 3.1 (adopted from [70]) General Fabrication Process 23

Figure 3.2 Molecular arrangement and planer zigzag conformation 24

Figure 3.3 DMF Molecular arrangement 25

Figure 3.4 Acetone molecular arrangement..... 26

Figure 3.4 Spin-Coating Device at Micro and Nano Device laboratory, Concordia University 28

Figure 3.5 Evaporating Machine at Micro and Nano Device Lab, Concordia University 29

Figure 3.6 FTIR device at Concordia Center for Composites, Concordia University 31

Figure 3.7 SEM Device at Thermodynamics of Material Research Lab, Concordia University 32

Figure 3.8 Confocal Microscope at Thermal Spray and Multiphase Flow Laboratory, Concordia University 33

Figure 4.1 Microfabrication process of PVDF-TrFE thin film. 37

Figure 5.1 SEM micrographs of the PVDF-TrFE films (a) without post-thermal annealing; with post-thermal annealing at: (b) 30 °C, (c) 50 °C, (d) 70 °C..... 40

Figure 5.2 FTIR spectra of all the prepared samples	43
Figure 5.3 Effect of spin coating speed and annealing temperature on the formation of β -phase in the PVDF-TrFE film.....	43
Figure 5.4 Comparing the thickness test results with FTIR results.....	44
Figure 5.5 Effect of the number of polymer layers on the formation of β -phase in the PVDF-TrFE film...	45
Figure 5.6 Effect of the addition of $Mg(NO_3)_2 \cdot 6H_2O$ on the formation of β -phase in the PVDF-TrFE film.	46
Figure 6.1 Experimental setup for sample testing.....	48
Figure 6.2 frequency and amplitude of applied point load (the vertical title is force in N)	49
Figure 6.3 Output voltages for each sample (top red sinusoidal waves which their amount and units are expressed on the right vertical axis) as a result of equal applied sinusoidal force (bottom blue sinusoidal waves at the same conditions and same amount which are demonstrated on the left vertical axis)	51
Figure 6.4 Effect of Annealing Temperature on generated output voltage in the piezoelectric generation characterization test	53
Figure 6.5 Experimental setup to record generated voltage due to applied point force.....	55
Figure 6.6: Geometry of 5x5 mm samples with two Al electrodes at top and bottom and a layer of Piezoelectric PVDF polymer in the middle as a sandwich structure in COMSOL.....	57
Figure 6.7 A zoomed-in photo of a sample with PVDF thickness of 43-microns and two Al electrodes at its end (one of the four samples with different PVDF thicknesses that are modeled in Comsol)	57
Figure 6.8 Mesh structure and fine size of the samples according to the COMSOL sizing (the mesh size of all four simulated samples is the same).....	58
Figure 6.9 Stress results of the samples in 2D and 3D view: The load is applied in the middle of the top electrode as a point load (a point is designed on the middle of the top electrode, and then, a point load applied on that point).	59
Figure 6.10 The distribution of electric potential between electrodes of the samples and the amount of the potential difference is: (a) 699 mV for PVDF layer thickness of 43 microns, (b) 491 mV for PVDF layer thickness of 32 microns, (c) 179 mV for PVDF layer thickness of 16 microns, (d) 69 mV for PVDF layer thickness of 10 microns.	60
Figure 6.12 Relation between PVDF Thickness and output voltage of the samples	61
Figure 7.1 Effect of thermal annealing on average output voltage in experimental test	63
Figure 7.2 Effect of various fabrication factors on average V out according to the simulation.....	64

LIST OF TABLES

Table 2.1 Properties of piezoelectric materials	17
Table 4.1 Design of Experiment.....	36
Table 5.1 Thickness measurements.....	41
Table 6.1 maximum voltage of each sample under the same and equal sinusoidal point load	52
Table 6.2 Calculated g_{33} for each sample	56

LIST OF ACRONYMS

DMF	Dimethylformamide
EDXS	Energy-dispersive X-ray Spectroscopy
FTIR	Fourier Transform Infrared Spectroscopy
MIS	Minimally invasive surgery
PVDF	Polyvinylidene fluoride
RCA	Radio Corporation of America
SEM	Scanning Electron Microscope
TrFE	Trifluoroethylene

LIST OF SYMBOLS

E	Electric field	$[\frac{V}{m}]$
ε	Strain	-----
ε_r	Relative permittivity	-----
d	Piezoelectric strain constant	[C/N]
g	Piezoelectric voltage constant	[V-m/N]
P	Polarization	-----
σ	Mechanical stress	[Pascal]

Chapter 1

Introduction

1.1 Introduction

Among different transduction technologies such as piezoresistive, capacitive and piezoelectric, the piezoelectric polymer is the fittest material for numerous biomedical applications such as MIS instruments and catheters because of its biocompatibility. Using PVDF with its copolymer, TrFE, as a piezoelectric material is a common method of fabrication of a force, pressure or tactile sensor due to its ease of implantation and various fabrication procedures. However, PVDF films have been used as force/pressure sensors for many industrial applications as well.

1.2 Piezoelectric Effect and Polymers

Piezoelectricity is a reversible electromechanical effect that results in the accumulation of the electric charge in solid materials due to the applying of mechanical stress, and vice versa. It means applying an electrical input to piezoelectric materials results in inducing a mechanical deformation in the material, and applying stress (or strain) to the piezoelectric material results in the accumulation of the electric charge inside the material [1].

Piezoelectric materials have two different responses that can allow them to convert mechanical energy to electrical energy. The direct effect is when a force is applied to that piezoelectric material, while the secondary effect (converse effect) is when a voltage is applied across the piezoelectric material and causes the deformation. These two effects are shown in figure 1.2.

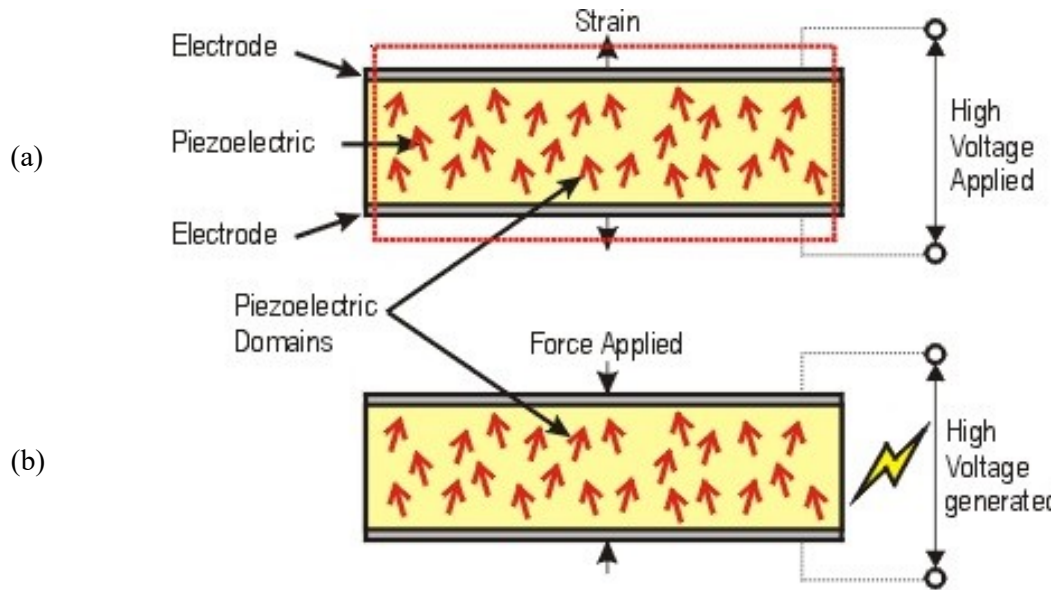


Figure 1. 1 (adopted from Azo Materials [2]) Direct and converse effect in piezoelectric materials. (a) When a voltage is applied across a poled piezoelectric device, the material expands in the direction of the field and contracts perpendicular to the direction of the field. (b) When a force is applied to the piezoelectric, an electric field is generated.

Polyvinylidene fluoride (PVDF) and its copolymer [PVDF Trifluoroethylene (PVDF-TrFE)] are of the main piezoelectric polymers used in different applications, such as beams, plates and membranes for vibration control, monitoring of the structure health, and force and pulse sensing. Good mechanical flexibility, biocompatibility, MEMS compatibility, and excellent sensitivity, particularly in harsh and biological environments, are the main properties of these polymer materials [3]–[7]. The capability of using these polymers under axial and normal tensions and stresses is the other property that makes these polymers a promising material for implementing in tactile force sensors.

In addition to the possibility of fabrication of the PVDF and PVDF-TrFE films, these films are commercially available in different thicknesses that can be used for rapid fabrication of the related devices. However, the main disadvantage of the piezoelectric sensors is that they are not sensitive

to low-frequency dynamic loads, and they can only be used for dynamic stimuli with high frequency. Moreover, since their sensitivity depends on the direction of the applied load, they are sensitive to external noise. Their other limitation is their sensitivity to temperature due to the pyroelectric effect, which cannot be separated from the piezoelectric effect [8], [9].

1.3 Pyroelectricity

In some materials, as the temperature changes, the polarization of the material is changed. This phenomenon is known as pyroelectricity. There are two main methods to measure the pyroelectric coefficient of a material. In the first one, the shape and dimensions of the material are kept constant while changing the temperature. In this method, the observed pyroelectric effect is known as the primary pyroelectricity. In the second technique, the material is allowed to change size and shape as a result of thermal expansion. The pyroelectric effect observed in this method is known as the secondary pyroelectricity, which results from piezoelectricity [10]. Figure 1.3 shows the pyroelectricity effect schematically.

In polymers, due to the existence of large thermal expansion coefficients and compressibility of these materials, pyroelectricity has higher importance than other materials such as ceramics. For materials showing pyroelectricity, the electric charge accumulation would be the result of the temperature effect. PVDF and PVDF-TrFE are well-known materials that show both piezoelectric and pyroelectric properties. The pyroelectricity in these polymers can be measured by the ratio of electrical charges delivered per unit of the area when the temperature changes by 1°C [11], [12].

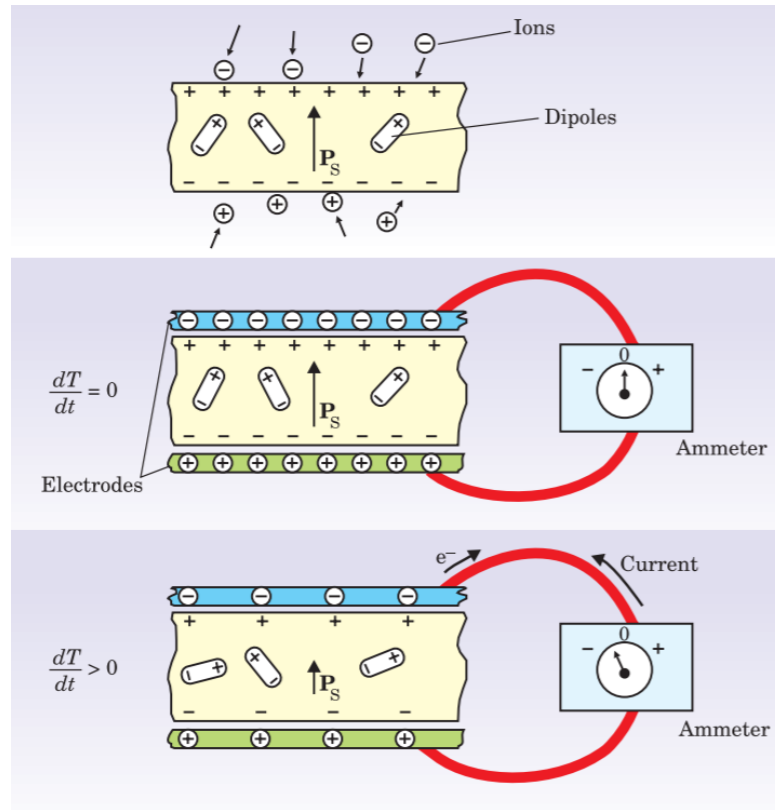


Figure 1. 2 (adopted from Lang [13]) “If a pyroelectric crystal with an intrinsic dipole moment (top) is fashioned into a circuit with electrodes attached on each surface (middle), an increase in temperature prompts the spontaneous polarization to decrease as the dipole moments, on average, diminish in magnitude. The horizontal tilting of the dipoles, pictured at the bottom, signifies the effect. Current flows to compensate for the change inbound charge that accumulates on the crystal edges.”

Pyroelectricity was found by the Greek philosopher Theophrastus about 2400 years ago, although piezoelectricity was observed in 1880 by Jacques and Pierre Curie [13], [14]. However, the technical applications of piezoelectricity were first introduced in 1920, and pyroelectricity was found two years later, in 1971, by Bergman et al. and by Nakamura and Wada [15]–[17]. As mentioned previously, PVDF is not the only polymer that benefits from these two properties, and these effects have been observed in other materials such as PVDF-TrFE, vinylidene cyanide, odd-numbered

nylons, and polyurea. However, PVDF and PVDF-TrFE have been used more widely in various applications.

1.4 Fabrication Processes and Deposition Methods

To obtain various structures of PVDF films (e.g., porous, dense, patterned, etc.), different techniques have been developed. Depositing methods such as spin coating, Langmuir-Blodgett, and solvent evaporation can be classified as the subcategory of the solvent casting technique. Although other processes such as electrospinning and soft lithography have been previously reported to fabricate PVDF thin films, in this work, only solvent casting methods will be discussed [18]–[20].

In the Langmuir-Blodgett method, applying a typical surface pressure of around $40 \frac{mN}{m}$ results in the assembly of the macromolecules and, consequently, the formation of a nanoscale polymer thin film. The main advantage of this method is a high control on the thickness of the film (at 2 nm). Spin coating is among the wet process methods, and thin thicknesses of polymers can be achieved by this technique. In the spin coating method, spin coating speed and time of deposition are the main two parameters that affect the final structure of the polymer. The main advantage of the solvent evaporation technique is its low cost. However, the final structure of this method is porous, which degrades the electrical and mechanical properties of the polymer.

1.5 Objective of the research

The objective of this research is to spin coat piezoelectric PVDF-TrFE polymer on a solid substrate effectively. To achieve this, the following steps/goals are required:

- a) Fabricate and characterize PVDF-TrFE piezoelectric films.

- b) Conduct an experimental procedure to identify the best condition for the fabrication of PVDF-TrFE films in order to obtain the best piezoelectric property.
- c) Deposit the materials (PVDF-TrFE polymer and Aluminum) layer by layer on a silicon substrate using the following steps:
 - 1) Deposition of an Aluminum electrode on a Silicon wafer using thermal evaporation technique.
 - 2) Deposition of the PVDF-TrFE film on the Aluminum electrode using the spin coating method.
 - 3) Deposition of another Aluminum electrode on the fabricated polymer films using thermal evaporation technique.
- d) Characterize the fabricated and spin-coated PVDF-TrFE, using scanning electron microscope (SEM), a confocal microscope and Fourier Transform Infrared Spectroscopy (FTIR)
- e) Experimental testing of samples to determine the output voltage due to applied dynamic loads.
- f) Evaluate the results by simulation.

1.6 Organization of the thesis

There are seven chapters in this dissertation, which are organized in the following format:

Chapter II briefly describes the available fabrication methods to produce PVDF-TrFE. Moreover, piezoelectricity and pyroelectricity properties are explained thoroughly in this chapter, followed by the explanation of the different phases in PVDF-TrFE and their properties. Furthermore,

the effect of experimental parameters such as thermal annealing, spin coating speed, the thickness of the film, polling, and the number of layers are discussed in this chapter.

Chapter III presents different materials and devices that are used for this experimental research.

In chapter IV, the technique to fabricate PVDF-TrFE piezoelectric film with great freedom in controlling the characteristics of the material is discussed in detail. The experimental results are discussed, and the effect of each parameter on the properties of the film is explained.

In chapter V, the optimum condition for the fabrication of PVDF-TrFE polymer is determined, and the characterization and morphology of samples are discussed.

Chapter VI studies the performance of the fabricated device. In order to do this study, the Bose machine is used to observe the produced signals of the various piezoelectric devices and compare them together.

In chapter VII, conclusions are summarized, and suggestions for future research are given.

Chapter 2

Literature Review: Piezoelectricity and Piezoelectric Polymers, Characteristics and synthesis Methods

2.1 Piezoelectricity

The prefix “piezo” comes from the Greek word pressure. The combination of the mechanical deformation in solid bodies and the electrodynamics of continuous media forms the piezoelectricity. Almost all piezoelectric materials show dielectric properties. The piezoelectricity effect inside the material occurs at speed much lower than the speed of light. The piezoelectricity property can be observed in both ferroelectric and non-ferroelectric states [21].

2.1.1 Direct and Converse Piezoelectric Effects

In non-centric crystals (and other similar structures), the piezoelectricity interaction between mechanical and electrical systems is linear. In the case of direct piezoelectricity, the change in the electric polarization of the material is proportional to the amount of force applied to the material. The piezoelectric coefficient (d) indicates the presence of piezoelectricity in a material. When mechanical stress of σ is applied to the piezoelectric material, the material gets polarized by the amount of P as shown in equation 1 [22]:

$$P = d\sigma \quad (1)$$

In the case of converse piezoelectricity, when an external electric field of E is applied to the material, it results in the production of a strain (ϵ) as:

$$\varepsilon = dE \quad (2)$$

Another parameter that should be taken into account when piezoelectric materials are being investigated is relative permittivity (ε_r). Relative permittivity is for a piezoelectric material is defined as the dielectric displacement per unit electric field.

Figure 2.1 shows the direct and converse piezoelectric effects, respectively. Both direct and converse piezoelectric effects can be used in various applications. Technical applications of piezoelectricity are shown in figure 2.2.

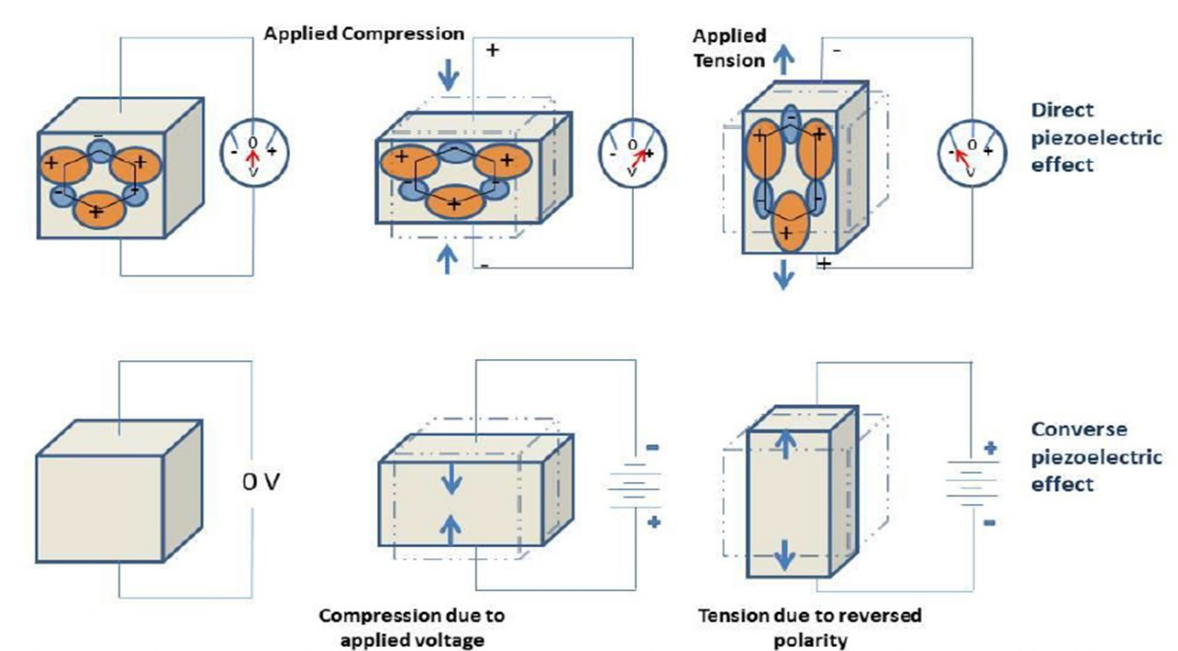


Figure 2. 1 (adopted from Tandon [23]) Direct and converse piezoelectricity.

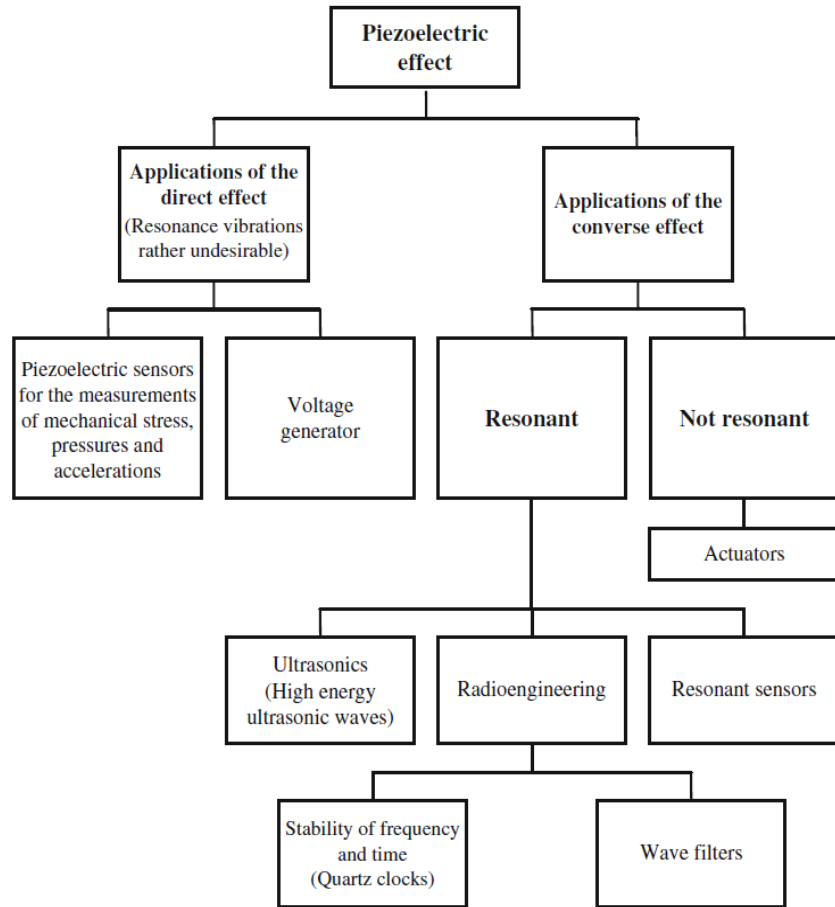


Figure 2. 2 (adopted from Tichy [24]) Applications of direct and converse piezoelectricity.

Due to the anisotropy in piezoelectric materials, coefficients are determined for each direction of the element. The piezoelectric coefficient ' d_{ij} ' determines the amount of generated charge in the material, in response to the applied stress or alternatively. It also shows the amount of strain experienced by the material per unit of the applied electric field. Here, 'i' represents the direction of the polarization (or applied electric field), and 'j' displays the direction of the applied stress (or induced strain). The subscript values 1, 2 and 3 show the orthogonal axes and 4, 5 and 6 denote rotation around their respective axes. Figure 2.3 illustrates the axis definition for piezoelectric constants. For instance, a "31" index represents an induced electric field between the two sides of the piezoelectric film, as a result of the mechanical stress applied along with axis number 1.

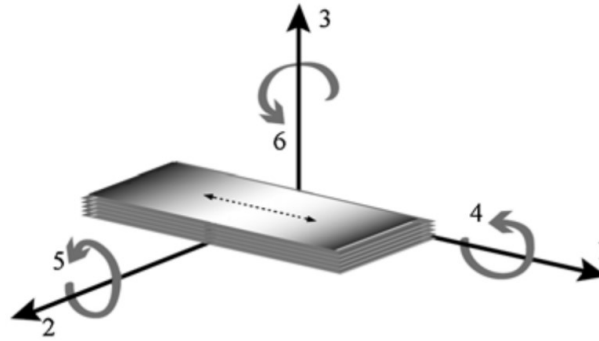


Figure 2. 3 (Adopted from [25]) Axis definition for the piezoelectric coefficients in different directions.

2.2 Piezoelectric Materials

As shown in figure 2.4, based on their physical properties, dielectric materials can be categorized into three main groups: that is, piezoelectric, pyroelectric, and ferroelectric materials. In dielectric materials, the exposure to an external electric field results in the production of electrical charge inside the material. Piezoelectric effect can be observed in dielectric materials that have lost their crystallographic inversion symmetry along a unique crystallographic axis. Pyroelectric materials benefit from spontaneous permanent dipole moments due to the spontaneous polarization changing with temperature. Ferroelectrics possess the same properties as pyroelectrics, with the only difference that in these materials, the spontaneous polarization can be reversed by applying an external electric field or mechanical stress [26].

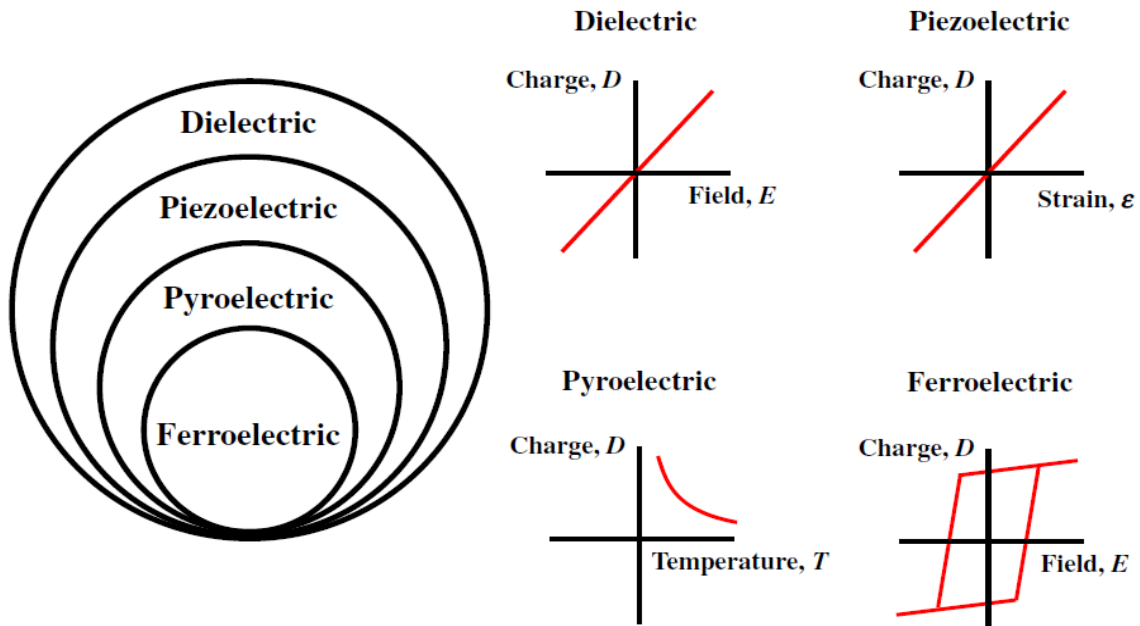


Figure 2. 4 (Adopted from Kim [26]) “The classification of insulator materials according to the physical properties.”

Bulk ceramics, ceramic thin films, multilayer ceramics, single crystals, polymers, and ceramics-polymer composites are the main types of piezoelectric materials. However, among all the known piezoelectric (and ferroelectric) materials, only very few of them are used in technical applications. The applicability of a material depends not only on the properties of the material but also, it depends on the desired application. For instance, for pressure, force, or accelerometer sensor, the material should have high piezoelectric coefficients (to be highly sensitive), high mechanical resistance and stiffness, low production cost, high insulation resistivity, high stability, easy processing, and linear relation between mechanical stress and electric polarization [24]. Each of these parameters can be found in various piezoelectric materials. In this part, a short description of some of the piezoelectric materials is provided.

2.2.1 Ceramics

2.2.1.1 Quartz

Quartz (SiO_2) single crystals are one of the main ceramics used in measuring devices. α -quartz, which is produced in low temperatures (under 573°C), is mainly used in piezoelectric applications. This material has a high resistivity to most of the acids and bases, and it is insoluble in water. At 573°C , phase transition happens, and by increasing the temperature, α -quartz is changed to β -quartz. Piezoelectric resonators and transversal or shear mode sensors are mainly made from the β -quartz [27], [28]. Gallium orthophosphate (GaPO_4), berlinite (AlPO_4), and langasites (LGS's) are the other crystals that have the same crystallographic symmetry as α -quartz. These homeotypic crystals can be used in applications with higher temperatures [29].

2.2.1.2 Barium Titanate (BaTiO_3)

The ferroelectric property of BaTiO_3 is known since 1946 when it was discovered on ceramic samples. This material undergoes four-phase transitions:

1. paraelectric cubic above the Curie temperature 120°C
2. tetragonal between 5 and 120°C
3. orthorhombic between -90 and 5°C
4. rhombohedral below -90°C

BaTiO_3 has mainly used multilayer ceramic capacitors and in positive temperature coefficient elements [30].

2.2.1.3 PZT Ceramics

Lead-zirconate-titanate (PZT) ceramics have significant piezoelectric properties and a reasonable price, which have led them to be used in a large variety of applications. The

crystallographic structure of these materials is perovskite, and under the curie temperature, they show ferroelectric properties. For commercially produced PZTs, the curie temperature is between 150 to 360°C. Above the curie temperature, the crystallographic structure changes to isotropic, and as a result, it is not piezoelectric. Consequently, the main limitation of these ceramics is the lack of high-temperature applications. In these materials, the chemical composition can be tuned by adding different amounts of elements such as Nb, Sr, Fe, Mn, and Cr to meet the specific application. The most common method to produce PZT ceramics is powder metallurgy. This method allows one to change the chemical composition of the material by adding powders of the additive materials, and it benefits from high scalability. These materials are mainly used as transmitters and receivers in ultrasonic sensing applications. However, it is difficult to fabricate them in miniaturized circuits [31], [32].

2.2.2 Polymers

2.2.2.1 PVDF and Its Blends with TrFE

From the first time in 1969 that the ferroelectricity effect was discovered in PVDF, a huge number of experiments have been performed on this polymer. This thermoplastic polymer has a high resistivity to harmful chemical substances and has a low value of the acoustic impedance, which allows it to be used in applications such as ultrasound imaging transducers [33]. Another interesting application of PVDF and its copolymers is in the musical instruments' pickups. These piezoelectric pickups benefit from a very low Q-factor; they do not have their own resonance (as in ceramic pickups), and therefore there is virtually no distortion of signals [34]. TrFE is the main copolymer that is used with PVDF, and both PVDF and PVDF-TrFE polymers are commercially available in the market.

Due to the presence of fluorine atoms, PVDF and its copolymers are highly polar. Depending on the processing method of this polymer, five phases of α , β , γ , ε , and δ can exist. However, α and ε phases are non-polar; due to the antiparallel packing of the dipoles. The polymerized monomer of $(-\text{CH}_2-\text{CF}_2-)_n$ exists in all the phases. The dipoles at the C-F bonds could either compensate each other in the molecule structure (e.g., in α -PVDF) or result in macroscopic dipole moment (e.g., in β -PVDF). Although α -PVDF is easy to obtain, however, from the point of view of macroscopic dipole moment, polar β -PVDF is the most important phase. It has been shown that the unique ferroelectric properties of these polymers originate from the orthorhombic polar all-trans (TTT) β crystalline phase [35], [36].

It should be noted that the crystallinity of the structure plays a vital role in the alignment of the dipoles. As the ratio of the crystallinity increases, dipoles get better alignment and result in the effective macroscopic dipole in the polar β -PVDF. However, there is always some amorphous part that lowers the effective polymer ferroelectric performance. To increase the crystallinity ratio of PVDF, it is used in copolymers with TrFE in a certain range of its molar ratios. This copolymerization can result in increasing the crystallinity ratio to up to 90%, and as a result, better piezoelectric activity [24].

The chain conformation for α , β , and γ phases of PVDF are shown in figure 2.5.a. comparing the chain conformation of α and β phases, the all-trans planar zigzag conformation of β -PVDF can induce a significant dipole moment. By applying external additive dipole moment to the β -PVDF, a large amount of spontaneous polarization can be generated. Due to the existence of gauche bonds in every four repeated units, the piezoelectric properties of γ phases are lower than β [37], [38]. The dipolar moment per unit cell value for β -PVDF is around $8 \times 10^{-30} \text{ C m}$ [39].

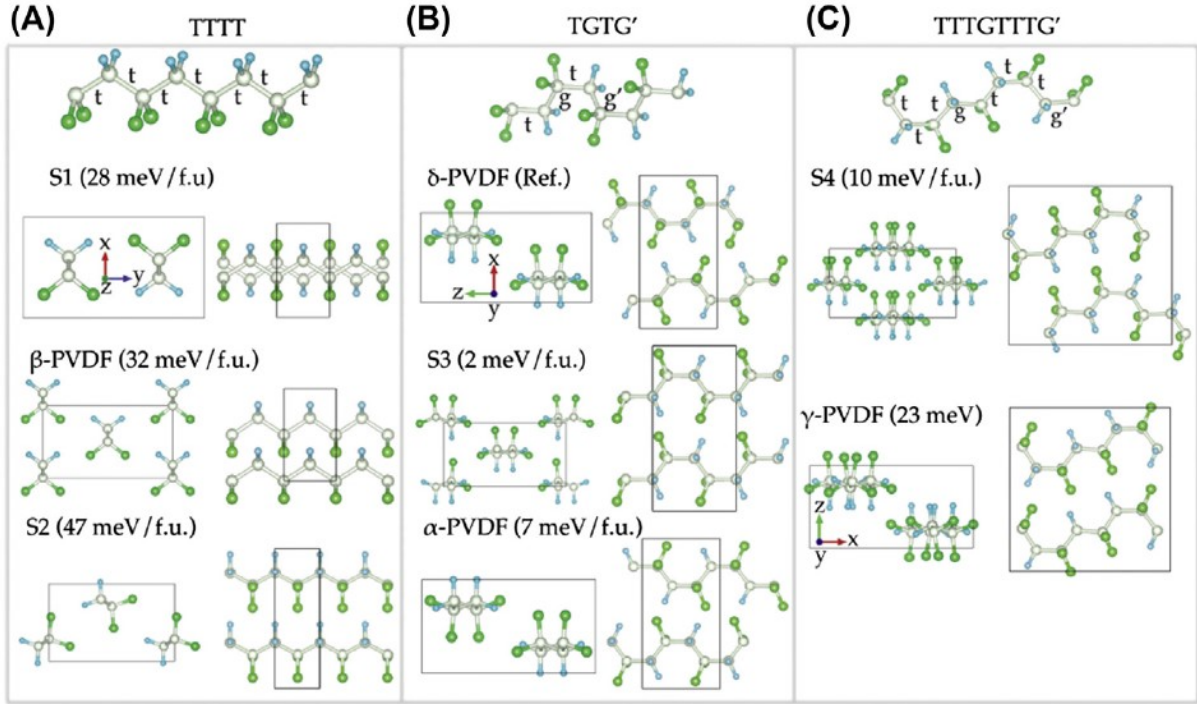


Figure 2. 5 (Adopted from Zhu [40]) Chain structures of α , β , and γ phases of PVDF.

Curie transition is defined as the transition from the ferroelectric β -PVDF to the paraelectric α -PVDF. This phase transition depends on various factors such as the polymer chain structure, processing condition, and posttreatment. Since by increasing the amount of β phase piezo-, pyro-, and ferroelectric properties are enhanced, it is favorable to have a phase transition that leads to the highest amount of β -PVDF. Due to the simple composition of PVDF-TrFE polymers, the mobility of the chain and conversion from one crystal phase to another are easily reachable. Different processes for changing and conversion from one phase to another one are shown in figure 2.6. However, excessive exposure of radiation to PVDF may damage its crystalline structure due to its high sensitivity; the crystal structure and different phases can be changed under a controlled condition, and piezoelectricity can be reached and induced [41].

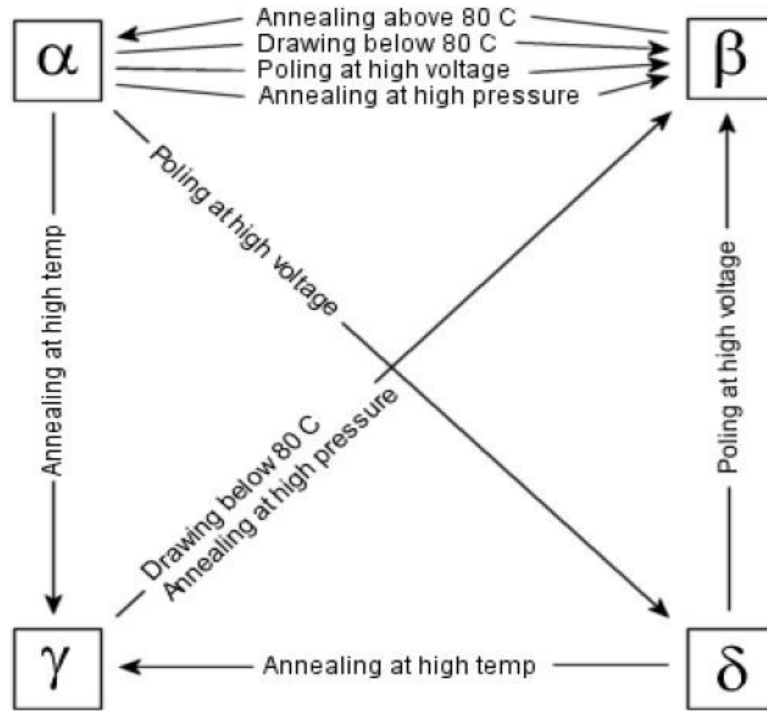


Figure 2. 6 (Adopted from Lovinger [42]) Transformation between the crystalline phases of PVDF.

To summarize this section, a summary of the piezoelectric coefficients of some common piezoelectric materials is shown in table 2.1.

Table 2.1 Properties of piezoelectric materials

Material	Relative Permittivity (ϵ_r)	$d_{ij}(\text{pC N}^{-1})$
PVDF	6-12 [43]	$d_{31} = 8-22$ [33] $d_{33} = -24$ to -34 [44]
P(VDF-co-TrFE)	18 [45]	$d_{31} = 12-25$ [46], [35] $d_{33} = -25$ to 40 [35], [47]
P(VDF-co-HFP)	11 [48]	$d_{31} = 30$ [49] $d_{33} = -24$ [50]
P(VDF-co-CTFE)	13 [51]	$d_{33} = -140$ [52]

P(VDF-TrFE-CFE)	65 [53]	—
Polyurethane	6.8 [54]	—
Polyamide 11	5 [49]	$d_{33} = 4$ [49]
Polyhydroxybutyrate	2-3.5 [55]	$d_{33} = 1.6-2$ [56]
ZnO	—	$d_{33} = 12.4$ [49]
PZT	500 [57]	$d_{33} = 225-590$ [58]
BaTiO ₃	1200 [57]	$d_{33} = 191$ [59]

2.3 Fabrication Methods of β -phase PVDF

As mentioned previously, the β -phase of PVDF shows the best piezoelectric, pyroelectric and ferroelectric properties. To increase the fraction of this phase in the polymer, various techniques have been developed. Mechanical stretching, electrical polling, co-polymerization with a second monomer, blending with other polymers, and crystallization (from solution) at temperatures under 70°C are the main methods that can be used to obtain β -PVDF [46].

The formation of the non-polar α -phase is kinetically more favorable than the β -phase, although the β -phase is more thermodynamically polymorph. As shown in figure 2.6, electrical polling of the α -phase results in the transformation of this phase to the δ -phase, and then to the β -phase. Moreover, as shown in the figure, cold drawing of the α -PVDF or annealing it under high pressure can result in the direct transformation of this phase to the β -phase. Although the mentioned processes can result in obtaining the β -PVDF, various methods have been developed to enhance the β -phase formation. Copolymerization of PVDF with other polymers is the main method to enhance the β -phase formation.

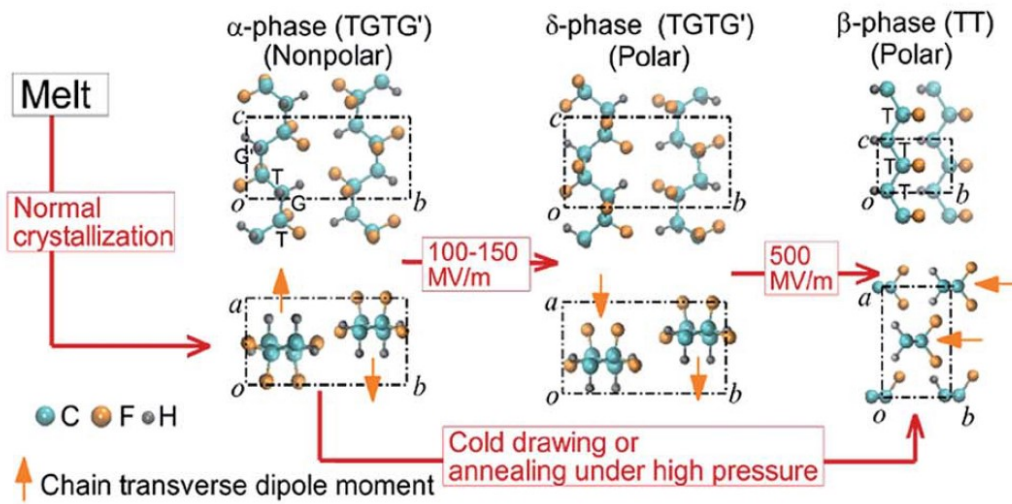


Figure 2.7 (Adopted from Yu [60]) “Phase transformation in PVDF polymer due to the electrical polling, cold drawing, and annealing under high pressure.”

2.3.1 PVDF Copolymers

As mentioned earlier, to enhance the properties of PVDF and respond to the technological needs, various copolymers of PVDF have been developed. Among these copolymers, TrFE is one of the main materials that has been investigated. PVDF-TrFE shows a Curie temperature lower than the melting temperature (contrary to what is happened in PVDF), which allows the phase transformation of ferroelectric to paraelectric [61]. In specific molar ratios, PVDF-TrFE always shows ferroelectric β -phase. In this material, the introduction of a third fluorine atom in the TrFE unit forces the polymer chains to align in an extended planar zigzag all-trans conformation below the Curie temperature when the percentage of TrFE is more than 11 mol% [62]. By increasing the amount of TrFE to more than 20 mol%, β -phase is formed independently of the processing condition and electrical polling [63].

As mentioned previously, when the polymer is heated above the Curie temperature, the ferroelectric β -phase converts to the paraelectric α -phase. This temperature defines the upper use temperature for piezoelectric and pyroelectric applications. Curie temperature for β -PVDF is

normally around 170°C. However, introducing a co-monomer to the polymer chains increases the inter-chain distance and dipolar mobility and, as a result, decreases the Curie temperature significantly [64]. For instance, in a previous study, it was shown that the Curie temperature for a 65/35 mol% PVDF-TrFE copolymer is 70-80°C [65]. Specifying the phase of the material can be performed using XRD analysis. In comparison, for another PVDF-TrFE copolymer made up of 73/27 mol%, the measured Curie temperature was 100-110°C. Reducing the amount of TrFE to 22 mol% has resulted in increasing the Curie temperature to 130-145°C. It should be noted that although reducing the amount of the copolymer material can result in increasing the Curie temperature, however, it decreases the amount of β -phase inside the material.

2.3.2 Solvent Casting

Solvent casting technique is one of the main methods to fabricate PVDF (and PVDF-TrFE) thin films. This technique includes all the deposit techniques such as spin coating, electrospinning, or solvent evaporation. Among these techniques, spin coating enables the scientists to fabricate thin films with various thicknesses and readily results in the formation of β -PVDF. For instance, a 2- μm PVDF thin film with a high β -phase content was fabricated using the spin coating technique by Benz et al. [66]. In their work, the solvent was created with a mixture of acetone and dimethylformamide (DMF), and it was coated on a single-crystal silicon wafer. Moreover, in work reported by Cardoso et al. [67], PVDF films with different β -phase contents are obtained just by varying the speed of the spinning and changing the post thermal annealing temperature.

In solving different amounts of PVDF-TrFE in various solutions, results change due to the material properties and quantity. Usually, N, N-dimethylformamide is acting as a solvent, but in some researches, it is reported that a mixture of DMF with Acetone (50:50) showed a better

response because acetone can vaporize sooner (volatile liquid) than DMF after deposition and help to make our fabricated sensor with lower porosity [68].

2.3.3 Effect of Thermal Annealing

After the spin coating process, PVDF films have porosities, which make it difficult to perform electrical polling. As a result, thermal annealing is applied to the fabricated polymers to reduce the amount of porosity. On the other hand, higher thermal annealing temperatures lead to smaller β -phase content and, therefore, the lower piezoelectric effect [44]. At thermal annealing temperatures equal to or higher than the Curie temperature, the β -phase content disappears. In this way, the piezoelectric response can be tailored depending on the application by applying controlled thermal annealing to the sample. However, deposition by spin coating imposes limits on the possible film thicknesses that can be obtained.

In another work conducted by Cardoso et al. [69], the effect of the post thermal annealing temperature on the piezoelectric properties of PVDF films has been studied. In their work, PVDF was coated in DMF solvent via a spin coater with 1000 rpm speed, and it was annealed in an oven at three different temperatures of 30, 50 and 70°C. It was concluded that although increasing the annealing temperature can result in decreasing the amount of porosity; however, it reduces the piezoelectric properties of the material, as well. This conclusion is also an agreement between other researchers in terms of the post thermal annealing effect.

Chapter 3

Instrumental and Experimental Procedure

3.1 Fabrication Process and Experimental Procedure

In order to measure the piezoelectric response and generally the sensor fabrication, it needs to sandwich a piezoelectric material like PVDF and its copolymer TrFE between two electrodes. First, a silicon wafer is needed for the substrate. For each sample, a 20*20 mm silicon wafer can be used. Second, a metallic alloy should be deposited on the silicon wafer (Metallization) as a bottom electrode. It can be Al, Cu, Au, or other similar ones. Although Au has better adhesion with PVDF-TrFE than Al as an electrode, a thin layer of Al is deployed and deposited by the Physical Vapor Deposition (PVD) method on a silicon wafer for this project due to its lower price and abundance compared to other metals.

The next step is the deposition of the PVDF-TrFE polymer via the spin-coating method. In order to test, analyze and compare the effects of various factors such as different solvents, additional hydrated salts, different spin coating speeds (3000 to 6000), and various annealing temperature treatment of the final device, numerous steps should have been done in the laboratory which will be discussed in the next chapter. Moreover, the concentration of PVDF-TrFE powder in the solution is also another variable factor that has a great impact on the final results and has an enormous effect on the piezoelectricity of the final device. These different fabrication conditions result in getting various piezoelectricity responses that make it easier for individuals to have a better understanding of the results. After the spin coating of PVDF-TrFE polymer on the bottom electrode, another Al layer is deposited on it as the top electrode and forms a sandwich structure. The reason for this consequent microfabrication process is to connect the piezoelectric response to

a circuit. Furthermore, for both electrodes (upper and bottom Al), a connecting wire needs to be attached to both sides separately in order to make it easier for further applications, which is another challenge during the fabrication process in this project.

In the end, final functions and treatments should be done to reach the project's desire. Having considered various factors, post-thermal annealing after spin-coating and polarization should be done to complete the fabrication process. Figure 3.1 summarizes the mentioned procedure and will be explained completely in the next chapters.

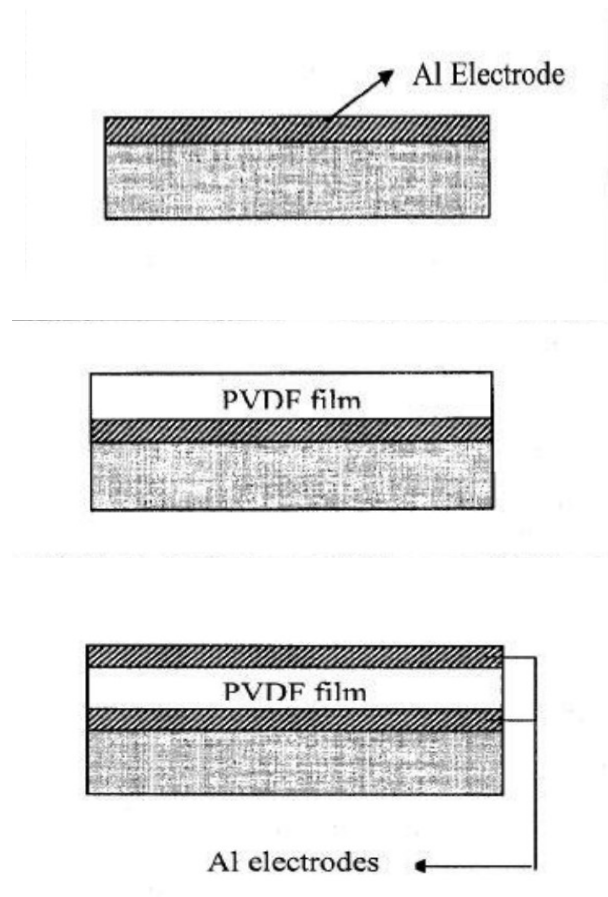


Figure 3.1 (adopted from [70]) General Fabrication Process

3.2 Materials Preparation

3.2.1 Polyvinylidene Fluoride-Trifluoroethylene (PVDF-TrFE)

PVDF-TrFE powder was purchased from Sigma-Aldrich Chemical Company (with technical product name of 900905 - Solvne®250/P300), and also, it can be called with its other synonym names like Fluoropolymer resin, P(VDF-TrFE), Poly(vinylidene fluoride-co-trifluoroethylene) with the composition of 25 mol % TrFE and 75 mol % VDF. Its linear chemical formula is $(C_2H_2F_2)_n(C_2HF_3)_m$, and the molecular arrangement can be understood clearly according to figure 3.2. As mentioned in Chapter 2, the dipoles at the C-F bonds could result in macroscopic dipole moment due to increment of the crystallinity ratio, and as a result, better piezoelectric performance could be obtained. Because of its planer zigzag conformation, dipole moment can be induced more easily than other conformations.

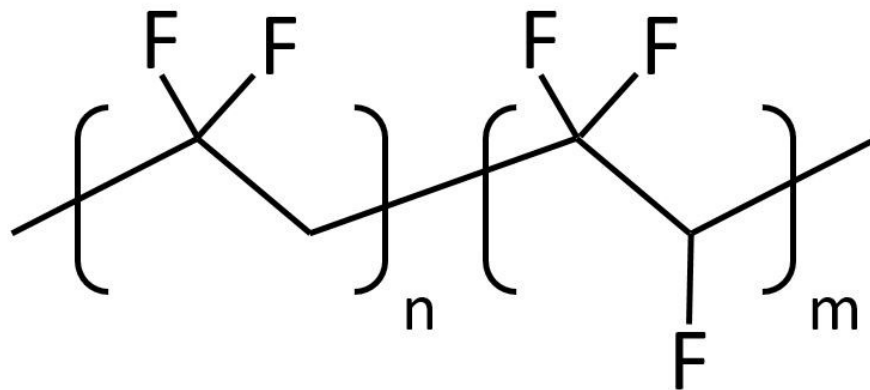


Figure 3.2 Molecular arrangement and planer zigzag conformation

Solvne® 250 P(VDF-TrFE) electro-active polymer is among the family of ferroelectric polymers, which combines magnificent electromechanical properties along with its easy processing behavior. Furthermore, its copolymers are inherently piezo-, pyro-, and ferroelectric,

which leads to enable applications such as printed memories, sensors, actuators, loudspeaker, acoustic transducers, energy harvesting devices.

In this project, Solvене® 250 P(VDF-TrFE) is used as a solute in the polymer solution for further deposition in order to test different experiments, which will be discussed in the next chapter. There are various types of PVDF-TrFE copolymers available in the market, but this one is the best fit for this research due to its molar composition rate between VDF and TrFE. Other similar products usually have a lower amount of TrFE, which is not desirable for this research according to the reasons discussed in Chapter 2.

3.2.2. N,N-Dimethylformamide (DMF)

N,N-Dimethylformamide (DMF) is served as one of the two solvents for the polymer solution preparation. DMF was purchased from Fisher Scientific Company (Acros Organics, analytical grade, CAS number of 68-12-2), and its molecular formula is C_3H_7NO with a molecular weight of 73.095 g/mol). DMF is a high boiling point polar solvent where its asymmetrical molecular arrangement can be seen from figure 3.3, and that makes it the desired solvent for PVDF and its copolymers because they are polar as well. Therefore, DMF is an excellent solvent for PVDF-TrFE in this research for piezoelectric thin film preparation.

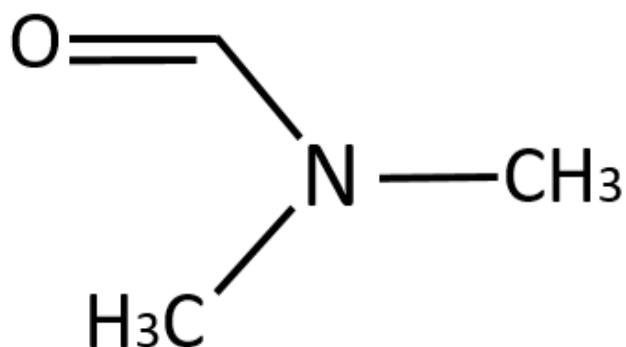


Figure 3.3 DMF Molecular arrangement

3.2.3. Acetone

Acetone is the other solvent purchased from Fisher Scientific Company (Acros Organics, analytical grade, CAS number of 67-64-1) in order to use for the polymer solution. The molecular formula of acetone is C_3H_6O , and it can be called by other names like 2-propanone, chevron acetone, dimethyl ketone, dimethyl formaldehyde, propanone and etc. This solvent has rather a high dipole moment that can be considered as a polar solvent, and it can be seen from its molecular arrangement according to figure 3.4. As mentioned in Chapter 2, acetone is a volatile liquid and can be vaporized sooner than DMF, which results in lower porosity [68]. Accordingly, a mixture of both DMF and Acetone is used for the solution preparation, and the procedure will be explained in Chapter 4.

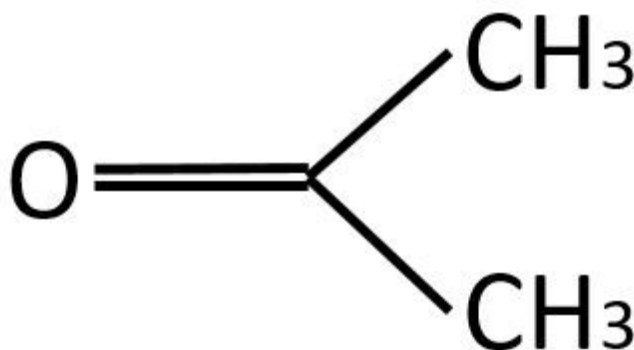


Figure 3.4 Acetone molecular arrangement

3.2.4. $Mg(NO_3)_2 \cdot 6H_2O$

In order to test the effect of additional hydrate salt on the piezoelectric properties of some samples, magnesium nitrate hexahydrate (Acros Organics, CAS number of 13446-18-9) was purchased from Sigma-Aldrich Chemical Company. Its linear formula is $Mg(NO_3)_2 \cdot 6H_2O$, and the

molecular weight is 256.41 g/mol. Studies have shown that the presence of some hydrate salts results in lower porosity, and as a consequence, higher piezoelectricity can be obtained [68].

These are the main materials purchased for this research, but some other minor and major stuff are also deployed in this experiment, which are already available at the MEMS Lab and Robotic Surgery Lab of Concordia University, and they will be explained in the next chapters.

3.3. Laboratory Sections, Devices and Procedures

3.3.1 Cleanroom and Spin-Coating Device

The aim of using an ordinary clean room in a laboratory is to prevent the outside environment from getting in because there may be some particles in the air leads to affect the experiment results. In the meantime, there are also other contamination sources threatening the cleanness of the lab environment. People and processes of the experiments can cause generating some contamination, which needs to be considered. Having known that, there are different levels and classifications of cleanroom for specific reasons. At Gina Cody School of Engineering Micro and Nano Device laboratory, there is a class 1000 cleanroom equipped with the necessary devices, which make the results of this research more reliable and accurate.

In this cleanroom, two main devices have been used regularly for this experiment. Oven and spin coating device are located at a class 1000 cleanroom to prevent the samples of this research from exposing to further environmental contamination. The spin-coating device (Laurell, North Wales, PA) can be programmed to rotate at various speeds from 500 to 6500 rpm and accelerate at a different rate to reach the desired speed. For example, in this project, droplets of the polymer are fallen on the substrate by using a syringe at 500 rpm for 15 seconds. After that, the device

accelerates and completes the spin coating process for the next 45 seconds according to the programmed speed.



Figure 3.4 Spin-Coating Device at Micro and Nano Device laboratory, Concordia University

3.3.2 Evaporating Machine

For the top and bottom electrodes, there is a need for a device to coat a thin layer of Al, Cu, or Au for the fabrication process. To this aim, an evaporating machine with physical vapor deposition (PVD) technique is used in the Micro and Nano Device Lab of Concordia University (figure 3.5). This device has six different vacuum motors to decrease the tank's pressure for the

deposition process. In the meantime, a small piece of metal (Al, Cu, or Au) is placed in a tiny basket made from a conductive wire that is connected to high voltages. Furthermore, the current can be controlled manually in the same way as the pressure. High current and low pressure inside the chamber cause the metal to evaporate and deposit a thin layer on the substrate, which is attached to the chamber's cap in an upside-down condition. After the deposition, the pressure should bring back to the normal ambient pressure and wait a couple of minutes to let the device cool down.



Figure 3.5 Evaporating Machine at Micro and Nano Device Lab, Concordia University

3.3.3 Wet Lab

A wet lab is used in order to prepare the polymer. There are sinks, Chemical fume hoods, and other facilities in the wet lab to make the experiment easier and safer. Furthermore, biosafety cabinets and hazardous waste tanks are available to prevent further infectious materials in other sections. Solvents and the powder solute are mixed under the fume hood while they are placed on

a magnetic stirrer device. The powder must add to the mixed solvent slowly because the risk of lump creation is high due to the PVDF-TrFE chemical properties.

3.3.4 FTIR Device

The Fourier Transform Infrared Spectrometer (FTIR) device is deployed for this research from facilities at Concordia Center for Composites (CONCOM). FTIR Analysis evaluates the infrared (IR) region of the spectrum, which has a lower frequency and a longer wavelength than visible light. It is also quantifiable in a sample when submitted to IR radiation. The fundamental explanation for this process is that the bonds among various elements absorb light at different frequencies. The light is evaluated by deploying an IR spectrometer, which generates the output of an IR spectrum. The infrared spectrum is a graph of IR light absorbance by the wavelength on the horizontal axis and the substance on the vertical one.

FTIR analysis is used in this experiment to evaluate the presence and amount of the β -phase PVDF. By getting all the prepared sample spectra, the difference in absorption peaks for various samples could be seen. Moreover, it could be concluded which sample has the best performance in terms of piezoelectricity and the presence of β -phase PVDF.



Figure 3.6 FTIR device at Concordia Center for Composites, Concordia University

3.3.5 SEM

Scanning Electron Microscope (SEM) is a type of electron microscope that is used to observe the fine structure of a specimen by scanning its surface with electron beams. These beams are focused and processed through the SEM column by getting use of different lenses and coils, which leads to interaction with atoms in the sample. These beams produce different signals that could be detected by an electron detector in the device, providing critical and important information about the morphology, topography and composition of the sample. Moreover, SEM has a greater depth of focus and provides stereoscopic information compared to optical microscopes, although its images are black and white.

In this research, different images from samples in various conditions are taken to compare them together and conclude a comprehensive result. For example, by increasing the temperature or increasing the layer of spin-coated PVDF-TrFE, the surface structural morphology of the

samples varies, which would be discussed in chapter 5. Figure 3.7 is the SEM device that is used for this project at the Thermodynamics of Material Research Lab, Concordia University.



Figure 3.7 SEM Device at Thermodynamics of Material Research Lab, Concordia University

3.3.6 Confocal Microscopy

Confocal microscopy or laser confocal scanning microscopy is under the optical microscope category with higher optical resolution and contrast rather than regular optical microscopes. These kinds of microscopes can be used in various industries such as semiconductor, life science, health care and material science, while the thickness test is important for this research. At Thermal Spray and Multiphase Flow Laboratory of Concordia University, there is an Olympus LEXT OLS4100 laser scanning confocal microscope that can do the thickness tests for all samples (Figure 3.8). Furthermore, these tests and their analysis will be discussed in chapter 5, and the impact of thickness on piezoelectricity will be demonstrated.



Figure 3.8 Confocal Microscope at Thermal Spray and Multiphase Flow Laboratory, Concordia University

Chapter 4

PVDF-TrFE Fabrication Process

4.1 Solution Preparation

In this work, the spin coating technique is used to deposit PVDF-TrFE thin films on the substrate. To prepare the solution for spin coating, PVDF-TrFE precursor solutions (10% W/V) were produced by dissolving PVDF-TrFE powder (Solvene R 250/P300, Sigma Aldrich) in a mixed solvent of DMF (Acros Organics, analytical grade) and acetone (Acros Organics, analytical grade) in 50:50 volume. Using a magnetic stirrer, the solution was mixed for 3 hours to ensure the homogeneity of the mixture. To investigate the effect of additional hydrate salt on the piezoelectric properties of the final polymers, 0.1% W/V of $Mg(NO_3)_2 \cdot 6H_2O$ (Acros Organics) was added to the sample that showed the highest amount of β -phase.

4.2 Substrate Preparation

To prepare the device, a piezoelectric thin film of PVDF-TrFE must be sandwiched between two parallel electrodes made from aluminum. To start the deposition process of aluminum, a silicon substrate was first cleaned using the Radio Corporation of America (RCA) technique, and then it has been placed in an evaporator machine to be coated with aluminum. For the evaporation process, a small piece of aluminum is placed inside the evaporation chamber, and the chamber is vacuumed. It is very important to create a high vacuum inside the chamber to avoid oxidization of aluminum during the evaporation. In this work, when the pressure of the evaporation chamber is reached to 10^{-6} Torr, the evaporation starts. By applying a voltage to the aluminum piece under the vacuum, it starts evaporating, and a thin layer of aluminum is coated on the silicon substrate.

4.3 Spin Coating

Solutions were spin-coated (Laurell, North Wales, PA) on the prepared substrates for 75 seconds. During this time, eight drops of the solution were put on the substrate. During the first 15 seconds, the substrate is spinning with the speed of 500 rpm, and then for 60 seconds, the speed increases to 5000 and 6000 rpm (depending on the sample).

4.4 Post Thermal Annealing

To reduce the amount of porosity in the deposited films, samples are annealed inside an oven. For this work, three different annealing temperatures of 30, 50, and 70°C were chosen, and samples were kept inside the oven for two hours.

At this stage, to investigate the effect of multi-spin coating on the morphology and piezoelectric properties of the thin films, some of the samples were again put inside the spin coater machine, and another layer of PVDF-TrFE was coated on them. Then, the post thermal annealing step was again repeated (at the same temperature). Table 4.1 summarizes the design of the experiment for the fabricated thin films.

In the last step, the samples are put again in the evaporator machine (with the same procedure) to coat the second layer of aluminum on top of the polymer film. Figure 4.1 shows the fabrication process schematically.

Table 4.1 Design of Experiment

	Annealing Temperature	Spin Coating Speed	Number of Polymer	Sample Name	
	(°C)	(RPM)	Layers		
10% PVDF-TrFE	30	5000	1	30-5k-1	
			2	30-5k-2	
		6000	1	30-6k-1	
			2	30-6k-2	
		50	5000	1	50-5k-1
				2	50-5k-2
	6000		1	50-6k-1	
			2	50-6k-2	
	70	5000	1	70-5k-1	
			2	70-5k-2	
		6000	1	70-6k-1	
			2	70-6k-2	

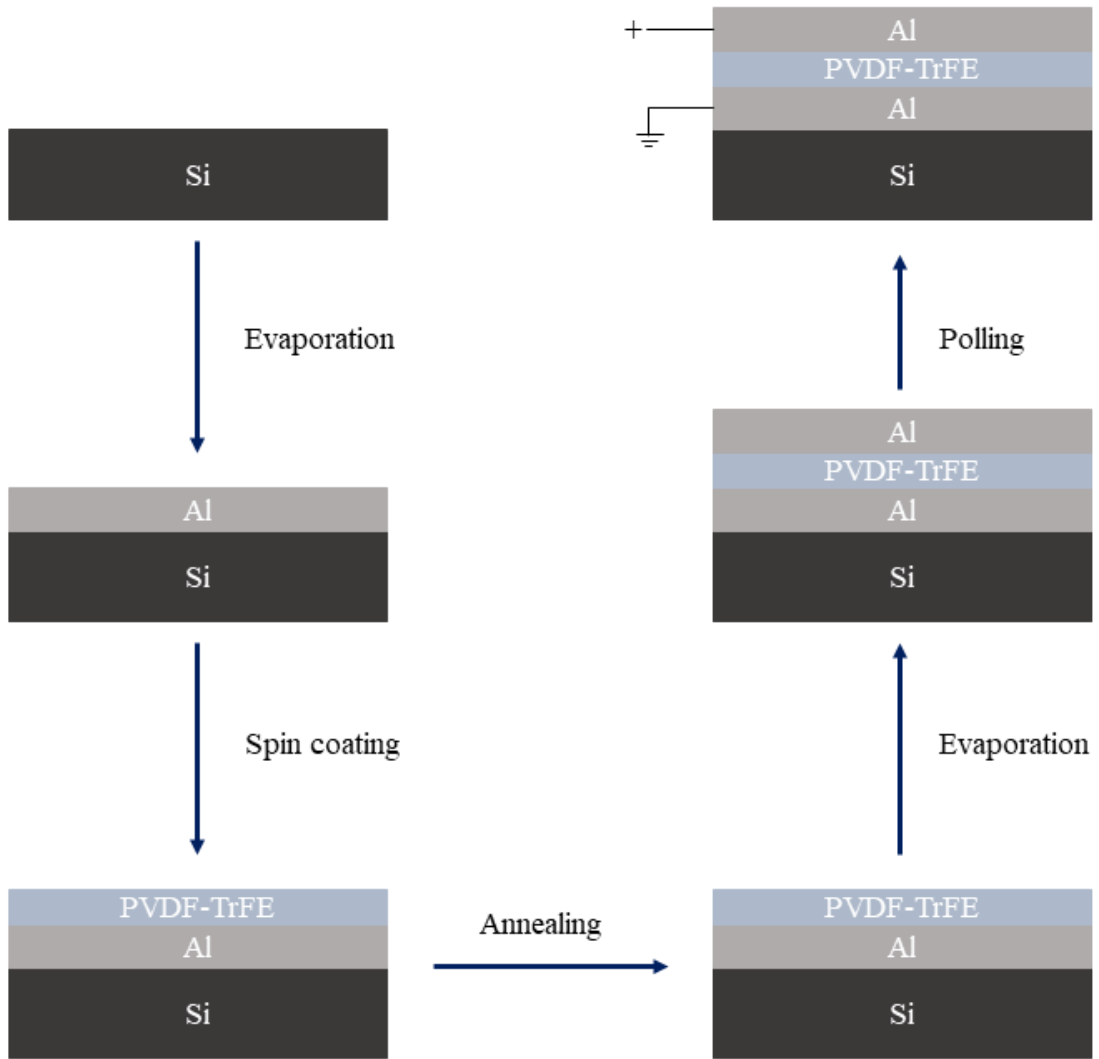


Figure 4.1 Microfabrication process of PVDF-TrFE thin film.

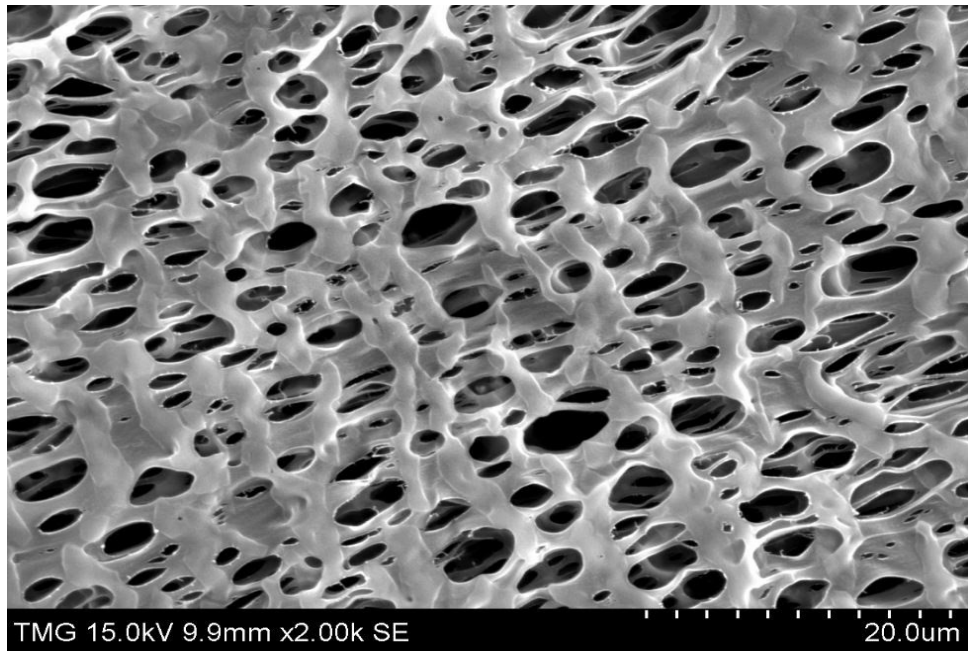
Chapter 5

Characterization of PVDF-TrFE Piezoelectric Polymer

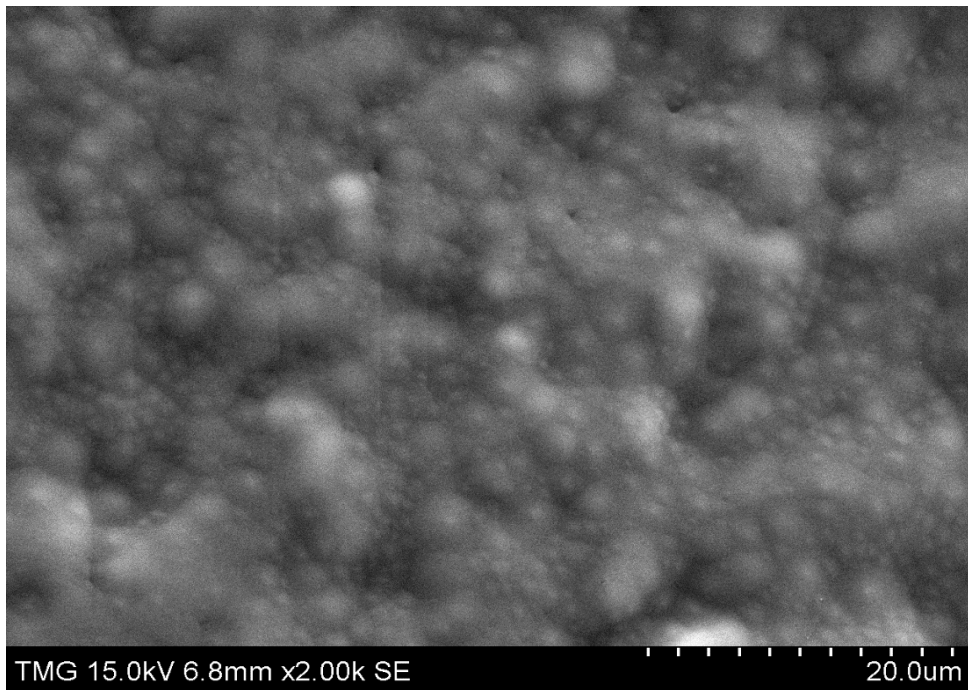
5.1 Effect of Post Thermal Annealing

As mentioned in chapter 2, at Curie temperature, the phase transition from β -phase to α -phase occurs. For the PVDF-TrFE polymer, this temperature is in the range of 57-79°C [49]. As a result, in order to maintain the β -phase, it is necessary to anneal the polymer below the Curie temperature. Moreover, annealing the polymer below the Curie temperature results in increasing this temperature to higher values. When the polymer is annealed below the Curie temperature, gauche defects from the ferroelectric phase are removed, and the degree of crystallinity and β -phase concentration in the polymer are increased. Furthermore, annealing results in reducing the amount of porosity in the polymer and vaporizes the solvent, which decreases the chance of interfering with the aluminum layers (on the bottom and top of the polymer) and creating a short circuit.

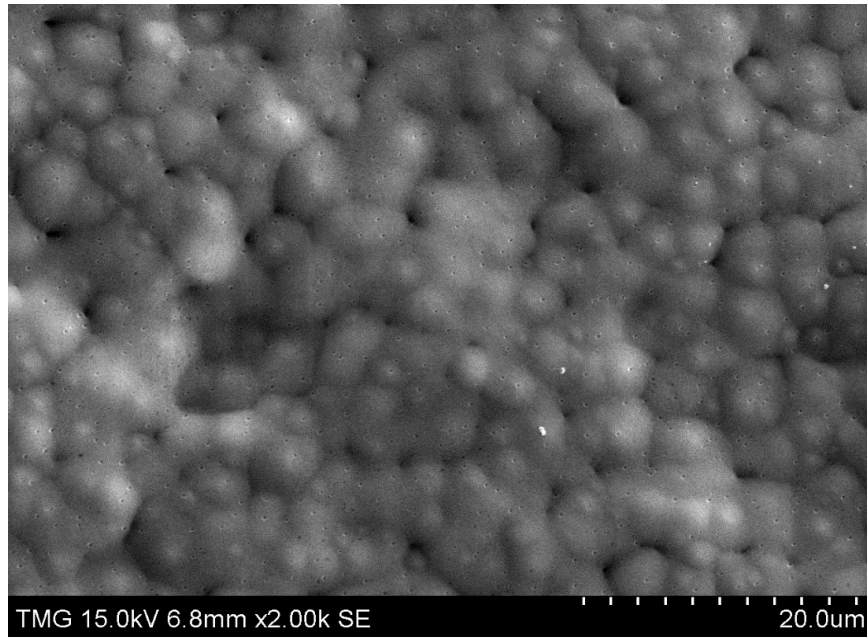
Figure 5.1.a shows the morphology of the fabricated PVDF-TrFE film without any post thermal annealing. As shown in the picture, the coated polymer has a lot of porosities (in μm range), and it is not suitable for coating the top electrode. However, as shown in figure 5.1.b-d, annealing the polymer is removing the porosities and results in a non-porous structure. Figures 5.1.b-d correspond to the samples annealed at 30°C, 50°C, and 70°C, respectively. Comparing the morphology of the annealed materials, it can be concluded that by increasing the annealing temperature, a finer structure with less amount of porosity can be obtained.



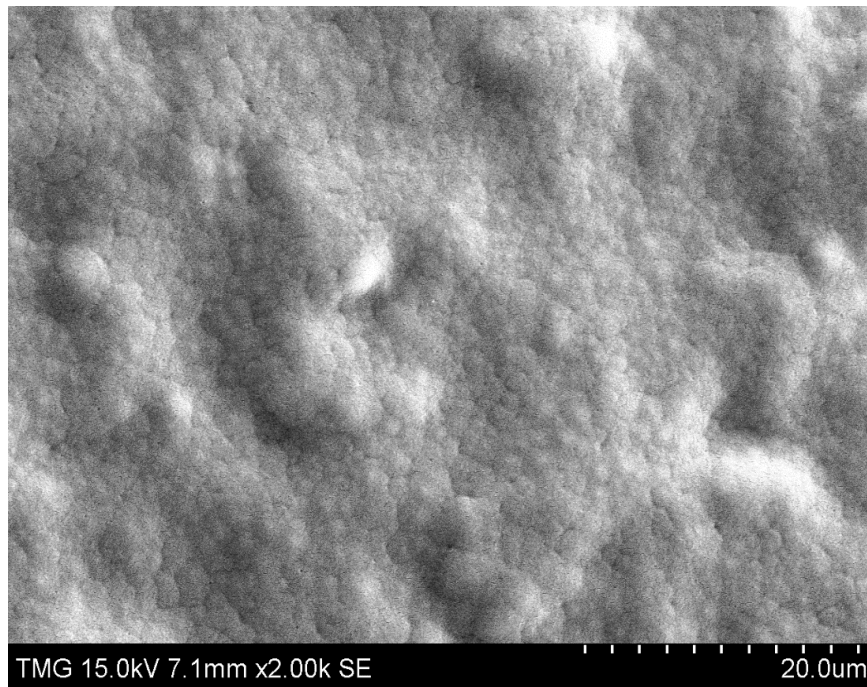
(a)



(b)



(c)



(d)

Figure 5.1 SEM micrographs of the PVDF-TrFE films (a) without post-thermal annealing; with post-thermal annealing at: (b) 30 °C, (c) 50 °C, (d) 70 °C.

As mentioned previously, one of the most important applications of post thermal annealing is to vaporize the solvent. Comparing the sample dried at room temperature (figure 5.1.a) with the annealed samples (figure 5.1.b-d), due to the slow evaporation rate of DMF and acetone in the non-annealed polymer, a porous structure is obtained. This structure is not favorable for the deposition of the conducting electrodes, and as a result, it hinders the polling process and the electroactive response of the material.

5.2 Thickness Test

To measure the thickness of the fabricated polymers, a laser scanning confocal microscope (Olympus LEXT OLS4100) was used. The detailed information about the thickness of the samples synthesized with 5000 and 6000 rpm spin coating speed and annealed in 30 and 70°C are reported in table 5.1.

As can be observed in the table, increasing the spin coating speed reduces the thickness of the final coating. Moreover, by increasing the annealing temperature, more solvent vaporization occurs, and consequently, the thickness of the polymer reduces.

Table 5.1 Thickness measurements

Spin coating speed (RPM)	Annealing Temperature (°C)	Min. Thickness (µm)	Max. Thickness (µm)	Average Thickness (µm)
5000	30	42.137	46.000	43.824
5000	70	14.609	17.705	16.100
6000	30	30.407	35.116	32.661
6000	70	9.993	13.094	10.967

5.3 FTIR Characterization

Figure 5.2 demonstrates the FTIR spectra of all the studied samples carried out in reflection mode. It is worth mentioning that the absorption peaks at 850 and 1275 cm^{-1} are associated with the formation of β -phase. These two absorption bands belong to the CF_2 symmetric stretching with the dipole moments parallel to the polar b axis [71]. As can be observed in the figure, increasing the annealing temperature has resulted in decreasing the amount of β -phase. Moreover, all the samples that were spin-coated with the rotation speed of 6000 rpm have shown a higher amount of β -phase comparing to those fabricated with the speed of 5000 rpm.

The effect of the spin coating speed on the amount of β -phase is shown in figure 5.3. As can be observed in the figure, for the same annealing temperature, the polymer fabricated with a higher coating speed is showing a higher amount of β -phase. The reason for this phenomenon is, for the same amount of solution, when the spin-coating speed increases, the thickness of the final coating is lowered. Moreover, as the speed increases, higher amounts of shear and elongation are applied to the polymer chain, which results in stretching the polymer during the spin coating process. This stretching results in superimposing the effects of solvent evaporation rate and promotes the α - to β -phase transformation [72].

Comparing the results obtained in the confocal laser test (table 5.1) with the FTIR results (figure 5.4) show that there is a complicated relationship between the fabrication parameters. For instance, although the sample 30-5k-1 has the highest value of thickness among the four studied coatings, however, it is showing higher amounts of β -phase compared to two of the samples. It can be concluded that the effect of the annealing temperature is more than the effect of spin coating speed. Although increasing the temperature can reduce the thickness of the polymer significantly; however, it prevents the formation of β -phase inside the material.

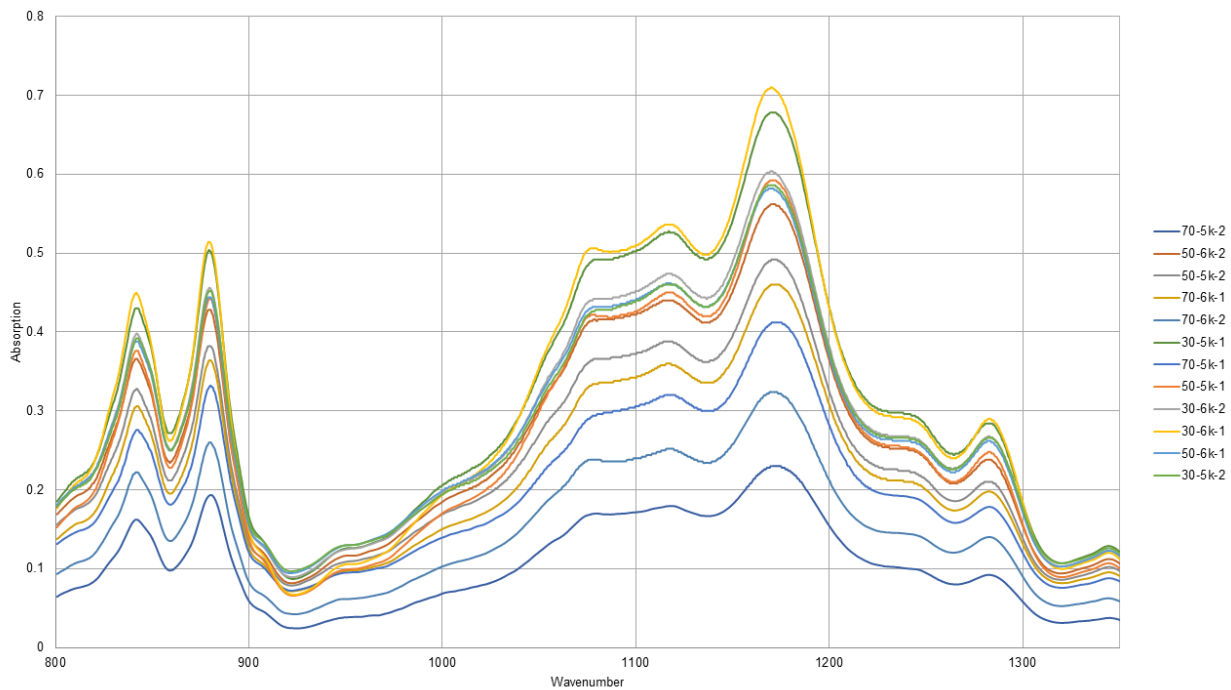


Figure 5.2 FTIR spectra of all the prepared samples

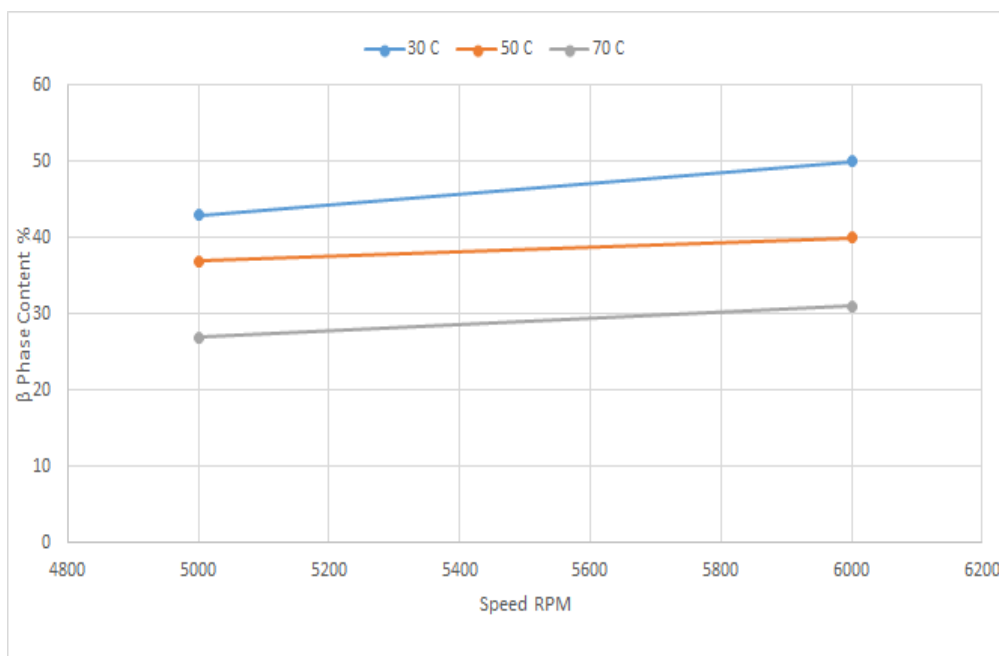


Figure 5.3 Effect of spin coating speed and annealing temperature on the formation of β -phase in the PVDF-TrFE film.

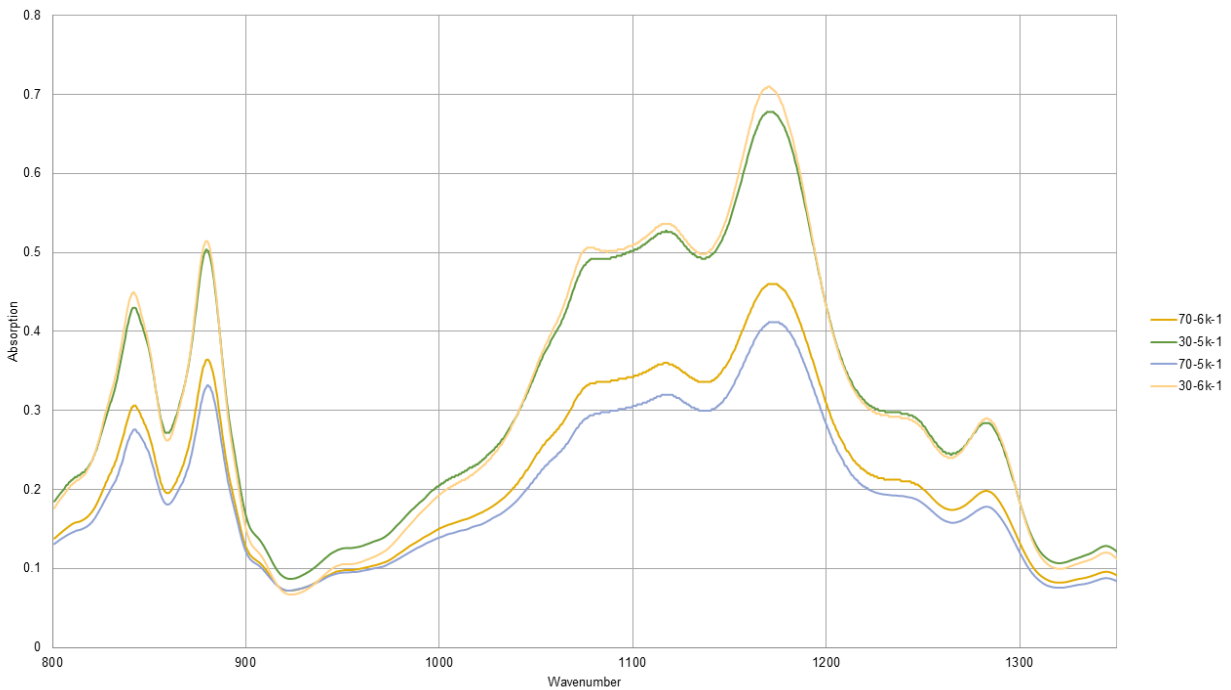


Figure 5.4 Comparing the thickness test results with FTIR results

Figure 5.5 shows the effect of the number of deposited layers on the amount of formed β -phase. As one can observe in the figure, all the samples that contain single-layer PVDF-TrFE show higher amounts of β -phase compared to the multi-layer samples. Although in the multi-layer structures, the size and number of porosities are reduced significantly, however, since the thickness of the sample is increasing (and piezoelectric properties have an inverse relationship with thickness), β -phase is reduced.

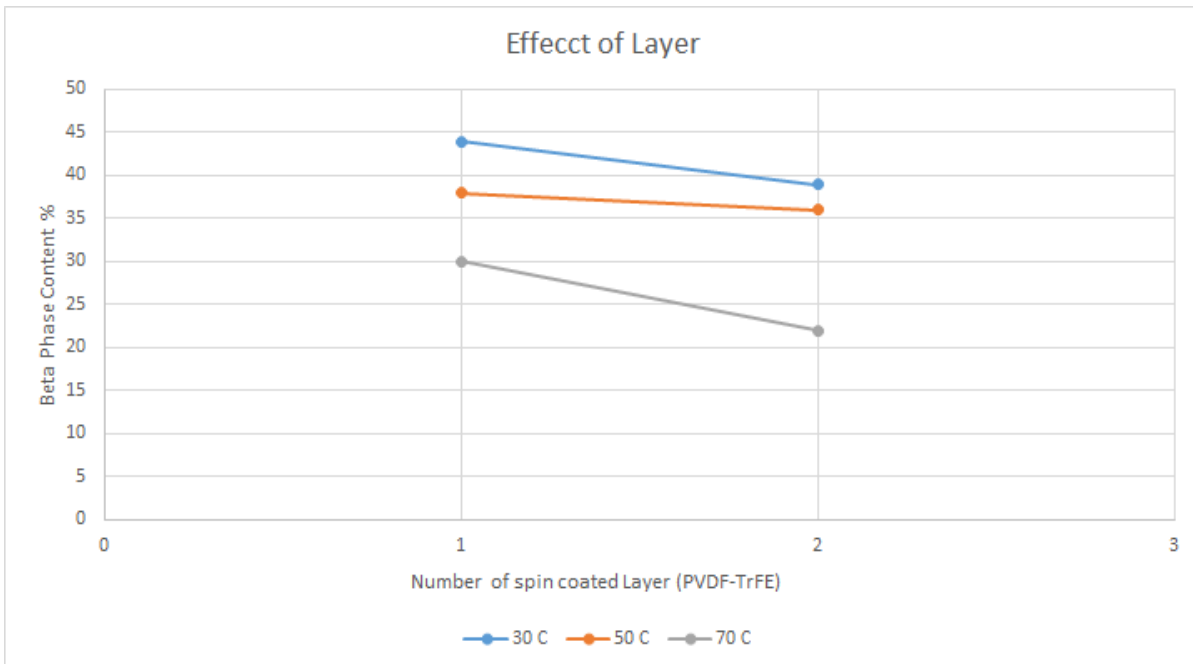


Figure 5.5 Effect of the number of polymer layers on the formation of β -phase in the PVDF-TrFE film.

5.4 Effect of Hydrate Salt

To investigate the effect of additional hydrated salt to the solution, 0.1% w/V of $Mg(NO_3)_2 \cdot 6H_2O$ was added to the solution, and the measurements were repeated for the sample, which has had showed the highest amount of β -phase (30-6k-1). The amount of salt was chosen based on a previously performed study [66]. As shown in figure 5.6, the addition of the hydrated salt in the casting solvent results in increasing the β -phase content through the polymer. It was also observed that adding the hydrated salt to the solution results in shifting the β -phase marker band near 1275 cm^{-1} slightly toward higher wavenumbers. These results are in agreement with the data obtained in other researches [66], [68].

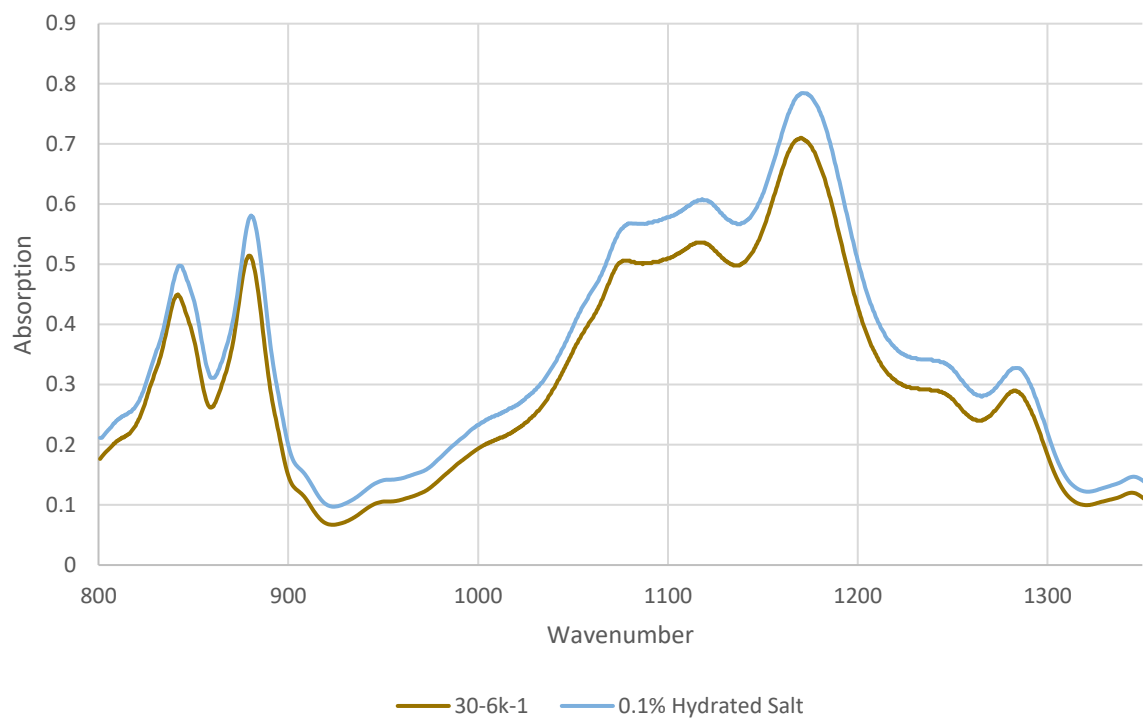


Figure 5.6 Effect of the addition of $\text{Mg}(\text{NO}_3)_2 \cdot 6\text{H}_2\text{O}$ on the formation of β -phase in the PVDF-TrFE film.

Chapter 6

Experimental Testing, Voltage Results and Computer Simulation

6.1 Experimental Setup

In chapter 5, characterization of PVDF-TrFE polymer was done, and the effect of thermal annealing, spin coating speed, additional hydrate salt and thickness of samples were investigated to see the amount of β -phase and morphology of those different samples. Therefore, in this chapter, those results should be verified by comparing their output voltage signals and see which one has higher sensitivity. Finally, it can be concluded whether they could confirm the characterization results of samples or not.

In order to investigate the polymer performance as a piezoelectric material, the piezoelectric generation characterization test must be performed. This test is a dynamic mechanical test where a dynamic load is applied to the sample. The available instrument at Concordia Robotic Surgery Lab is the Bose ElectroForce® 3200, which has the versatility of static to 200 Hz frequency response and can be used for a variety of biomedical research and engineered materials test applications.

To perform this test, the piezoelectric device is mounted onto the electroforce machine, and a predefined displacement is applied, while the total applied on the device is being monitored. At this point, by applying a dynamic load to the device (sinusoidal point load), the resultant electrical output signal of the device can be characterized. To have a clear and amplified voltage signal without noise, an oscilloscope and an amplifier are used during this process, and the experimental setup can be seen in figure 6.1.

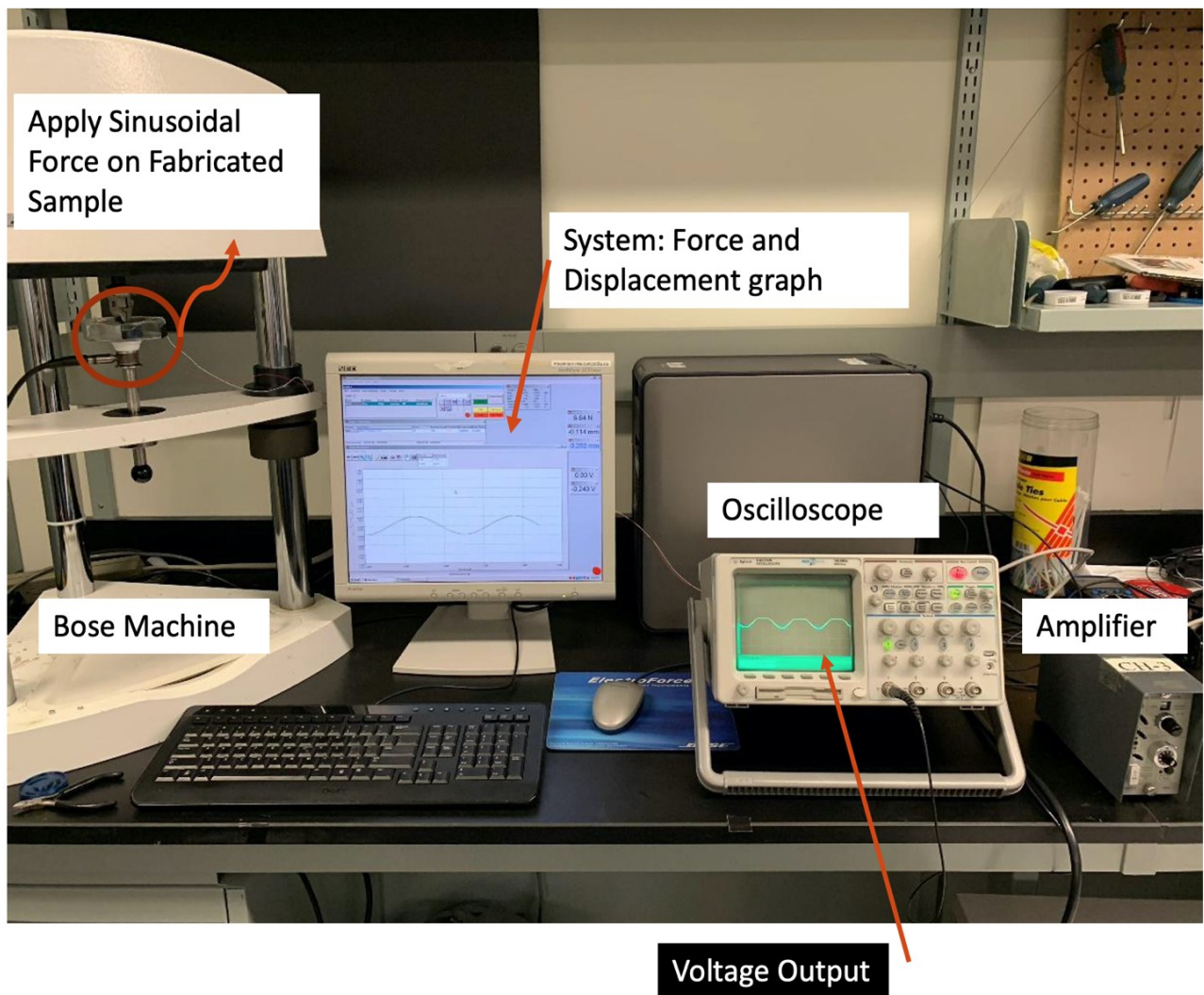
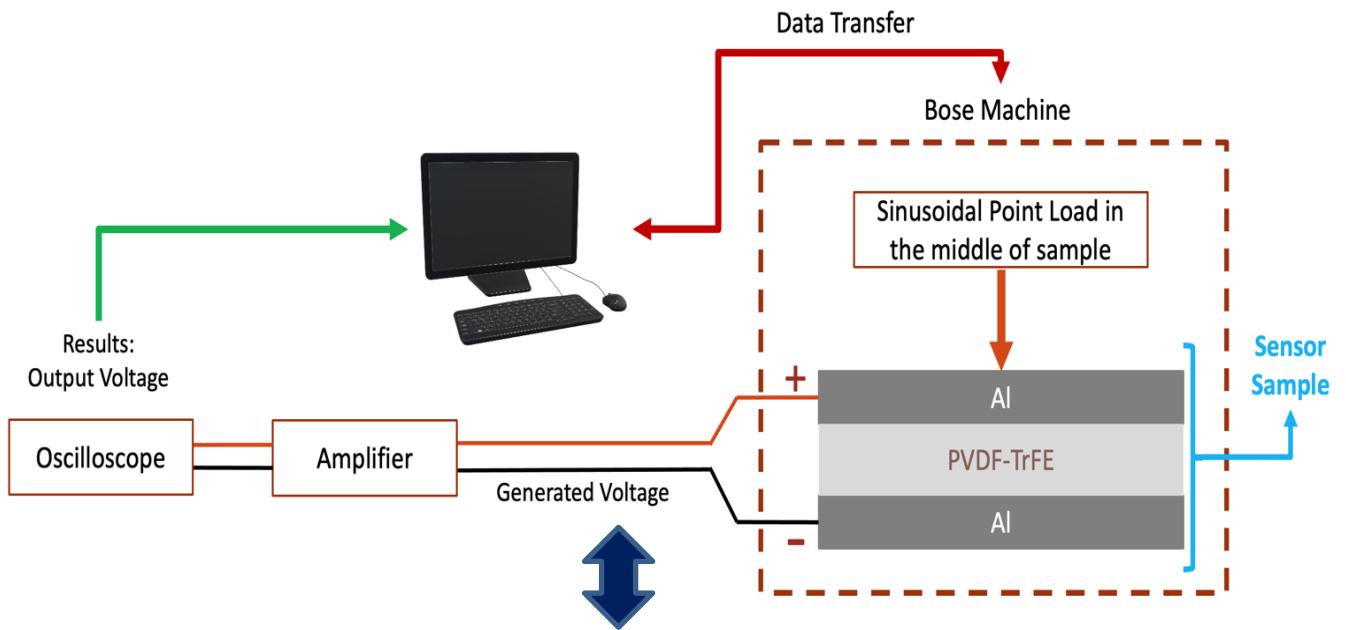


Figure 6.1 Experimental setup for sample testing

6.2 Applied Force and Output Voltage

By applying the same sinusoidal point force in the z-direction of the twelve fabricated experimental samples, their output voltages can be tracked and recorded. As illustrated in figure 6.2, the peak-to-peak amplitude of the force is -4.5 N from 0 to -4.5 N, and the negative mark represents the direction of the force, which is -z (this amount is chosen due to the sensor's potential application for biomedical devices such as end effector of a catheter). As a result, the generated piezoelectricity voltages show the same sinusoidal waveforms as well, and their ranges vary between 160 to 320 mV based on each twelve sensor samples. It can clearly be seen, according to figure 6.3, that when there is no force or is in its minimum amount (0 N), the output voltage does not show any potential differences between the sample's electrodes likewise. On the other hand, by increasing the force, the output voltage rises and shows its maximum amount (peak) exactly when the force is in its highest amount (-4.5 N). The relation between the applied force and output voltage for each sample is presented in 12 graphs in figure 6.3.

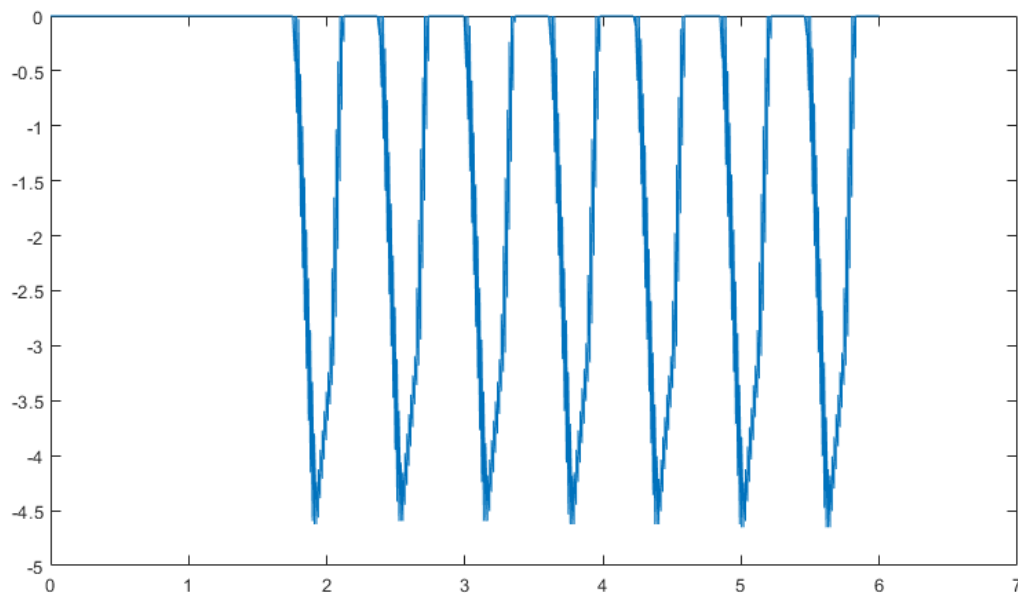
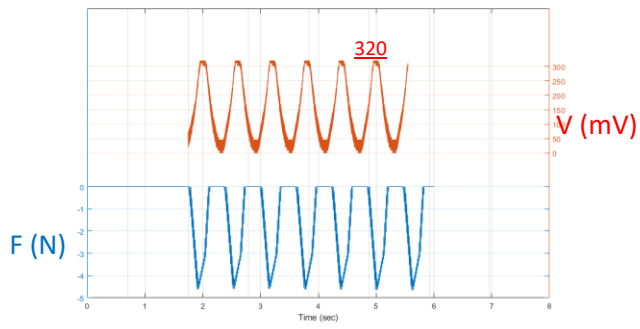
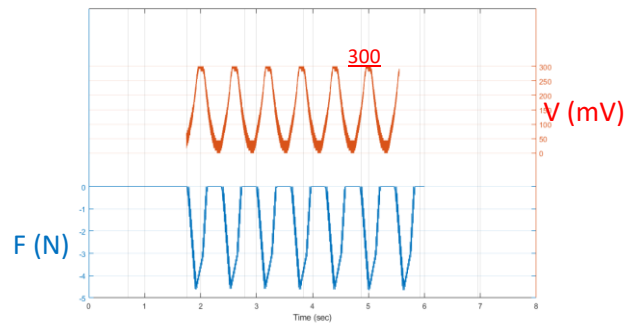


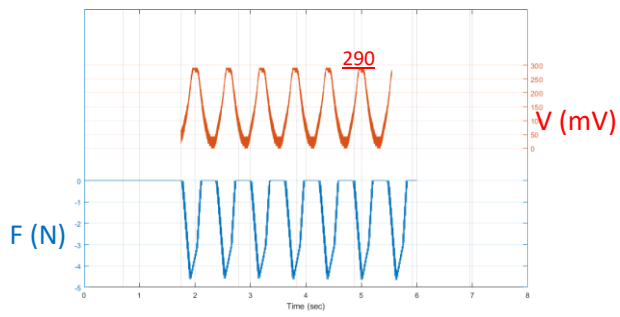
Figure 6.2 frequency and amplitude of applied point load (the vertical title is force in N)



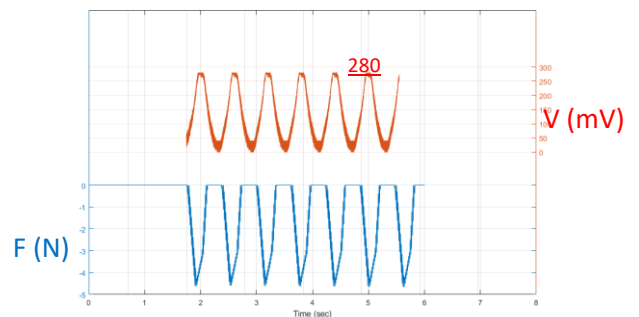
(1)



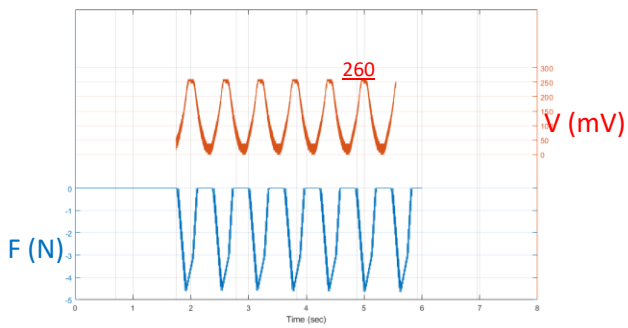
(2)



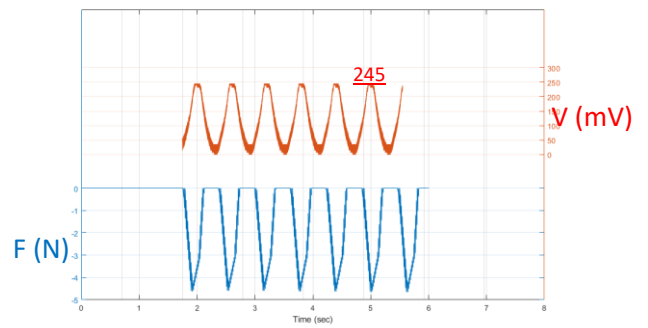
(3)



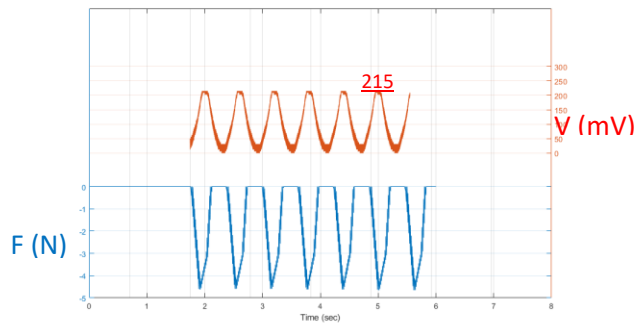
(4)



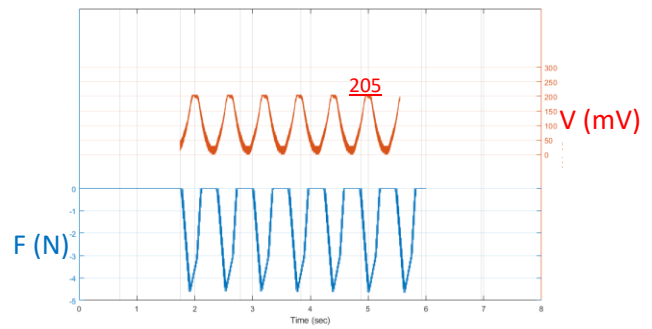
(5)



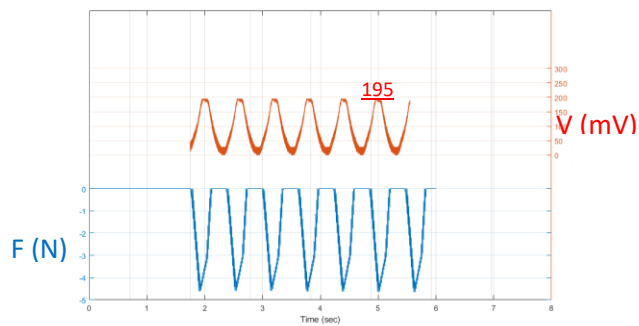
(6)



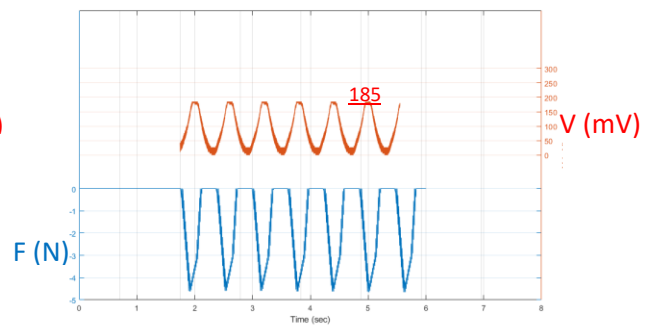
(7)



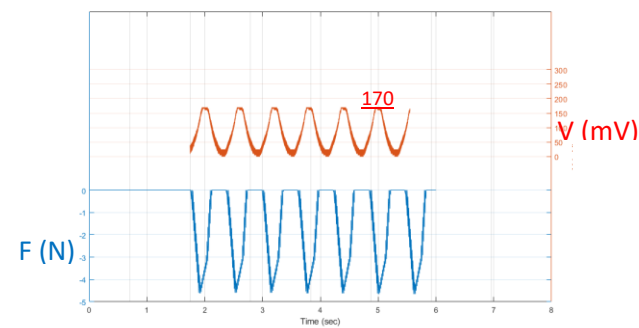
(8)



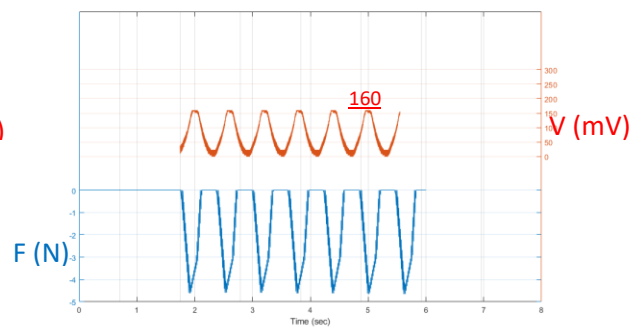
(9)



(10)



(11)



(12)

Figure 6.3 Output voltages for each sample (top red sinusoidal waves which their amount and units are expressed on the right vertical axis) as a result of equal applied sinusoidal force (bottom blue sinusoidal waves at the same conditions and same amount which are demonstrated on the left vertical axis)

6.2.1 Results and Analysis

By extracting the data from each signal, a clear data table with the maximum output voltage is established for all sensor samples. Table 6.1 shows the maximum generated voltage from the highest amount (which is assigned to sample number 1) to the lowest one (which is assigned to sample number 12). These sample codes in table 6.1 are the same as the code names for each sample where it was tested for piezoelectricity characterization and analysis in previous chapters.

Table 6.1 maximum voltage of each sample under the same and equal sinusoidal point load

Sample Codes	maximum force (N)	Maximum generated voltage (mV)
1: 30-6k-1	4.5	320
2: 30-5k-1	4.5	300
3: 30-6k-2	4.5	290
4: 30-5k-2	4.5	280
5: 50-6k-1	4.5	260
6: 50-5k-1	4.5	245
7: 50-6k-2	4.5	215
8: 50-5k-2	4.5	205
9: 70-6k-1	4.5	195
10: 70-5k-1	4.5	185
11: 70-6k-2	4.5	170
12: 70-5k-2	4.5	160

It can be concluded that lower annealing temperature leads to higher voltage and is considered more sensitive compared to those samples with higher annealing temperatures (figure 6.4). For example, in this experiment, the average output voltage for all the samples prepared with the same annealing temperature of 30 C is 297.5 mV, while it is 177.5 mV for samples with the same annealing temperature of 70 C in spite of other different fabrication factors.

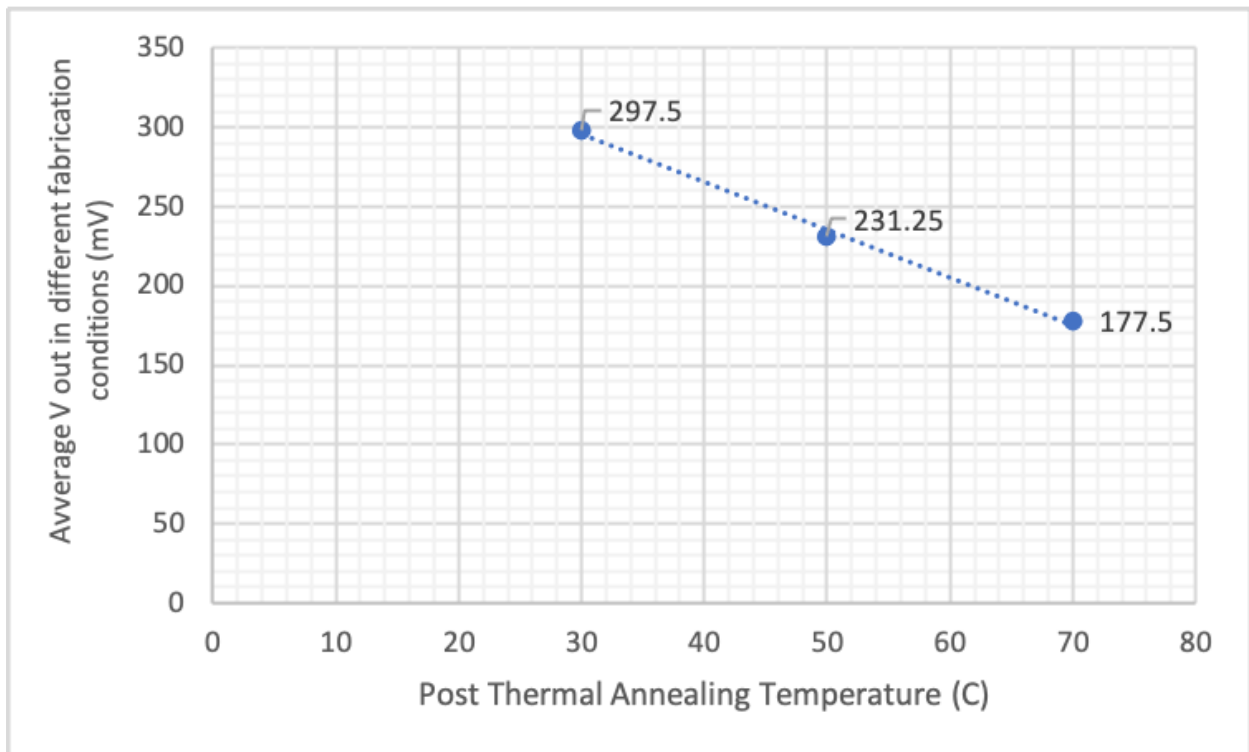


Figure 6.4 Effect of Annealing Temperature on generated output voltage in the piezoelectric generation characterization test

Furthermore, increasing the spin-coating speed of the device results in generating higher voltage output considering annealing temperatures are the same; however, a smaller number of fabricated layers has a higher effect on the piezoelectric voltage generation regardless of their spin-coating speed.

The number of layers and annealing temperature have a direct effect on the thickness of the samples. In chapter 5, it was observed that the annealing temperature has a higher impact on the morphology and thickness of the samples compared to the number of layers. Samples with higher annealing temperatures tend to have lower β -phase content, while their thicknesses are smaller (figure 5.3 and table 5.1). As a result, they were not considered as the best samples in this research in terms of piezoelectricity due to the FTIR characterization, and hence, this voltage test also confirmed the characterization analysis as well.

6.3 Piezoelectric Coefficient Calculation

Piezoelectricity has direct and converse effect, which was explained in chapter 2. For mathematical calculation and linking the electrical to/from mechanical properties, the piezoelectric coefficient is deployed in all studies. According to equation 3, piezoelectric material with a higher piezoelectric coefficient can generate a high electrical field [73]. Moreover, this coefficient can be named and calculated depending on testing conditions and various factors.

$$\text{Piezoelectric Coefficient} = \frac{\text{Electrical field}}{\text{Applied mechanical stress}} \quad (3)$$

Two main piezoelectric coefficients are expressed as d (piezoelectric strain constant) and g (piezoelectric voltage constant), which represent the relation between charge or electrical fields produced by applied mechanical stress (C/N or V/m over N/m^2) [73], [74]. The analytical calculations for these two formulas are described below:

$$d [C/N] = (\text{charge developed})/(\text{applied stress}) \quad (4)$$

$$g [V-m/N] = (\text{Electric field developed})/(\text{applied stress}) \quad (5)$$

A piezoelectric coefficient is numerically identical for both direct and converse effects. The piezoelectric coefficient, stress, strain, and induced charge are in three different dimensions, which were explained in chapter 2. In this research, according to the experimental approach and direction of applied point load (figure 6.3), piezoelectric voltage constant can be expressed by g_{33} and is obtained by formula six, which has direct mathematical relation with the output voltage [74]:

$$\frac{V}{T} = \frac{F \cdot g_{33}}{L \cdot W} \quad (6)$$

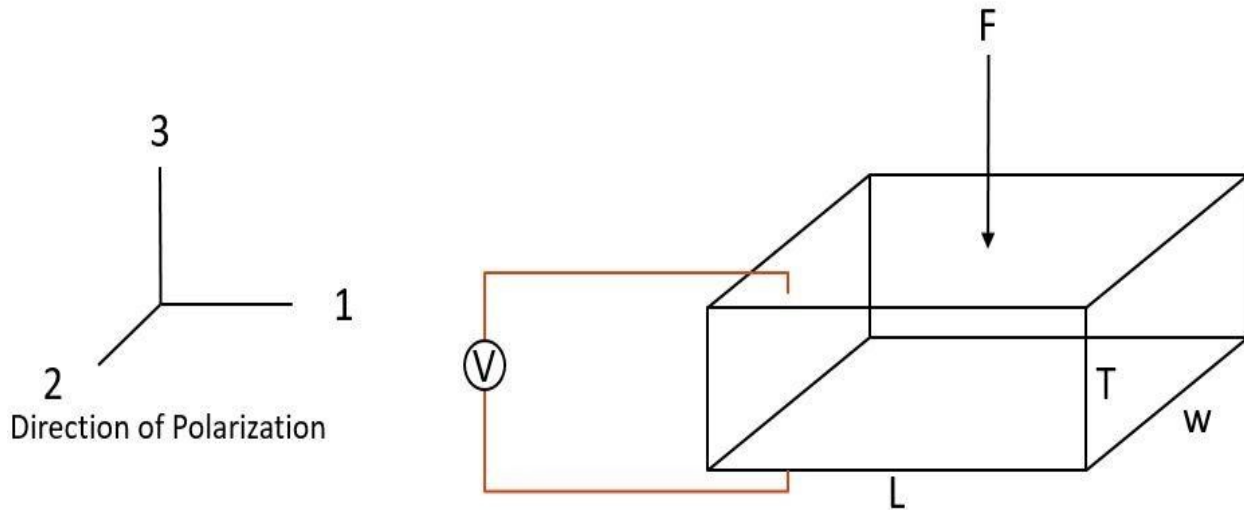


Figure 6.5 Experimental setup to record generated voltage due to applied point force

Table 6.2 demonstrates calculated g_{33} for each sample according to the discussed formula. Furthermore, Samples with higher g_{33} exhibit a higher piezoelectricity effect. Similar to the voltage result in section 6.2.1, the variation of the piezoelectric coefficient clearly confirms the FTIR characterization that determined the amount of β phase content. This means that samples with higher β phase content produce higher voltage and have higher piezoelectric constant.

Table 6.2 Calculated g_{33} for each sample

Sample Codes	max voltage (mV)	g_{33}
1: 30-6k-1	320	0.088
2: 30-5k-1	300	0.083
3: 30-6k-2	290	0.08
4: 30-5k-2	280	0.077
5: 50-6k-1	260	0.072
6: 50-5k-1	245	0.068
7: 50-6k-2	215	0.06
8: 50-5k-2	205	0.057
9: 70-6k-1	195	0.054
10: 70-5k-1	185	0.051
11: 70-6k-2	170	0.047
12: 70-5k-2	160	0.044

6.4 Computer Simulation with COMSOL

6.4.1 Device Modelling and Simulation Setup

In this study, the Piezoelectric Devices module of COMSOL Multiphysics is used to model and simulate a piezoelectric sensor based on PVDF polymer. The model consists of a PVDF layer defined as a piezoelectric material while it is sandwiched between two layers of Aluminum

electrodes. This means that on the top and under the bottom of the PVDF layer, a thin film of Aluminum is placed on both sides with the same thickness of 5 microns; however, the thickness of the middle layer (PVDF) varies from 10 to 43 microns in order to study thickness effect on piezoelectricity (4 samples with various thicknesses). Furthermore, the length and width of the modeled sensor are 5 mm, and they are shown in Figures 6.6 and 6.7 as examples of the sensor geometry.

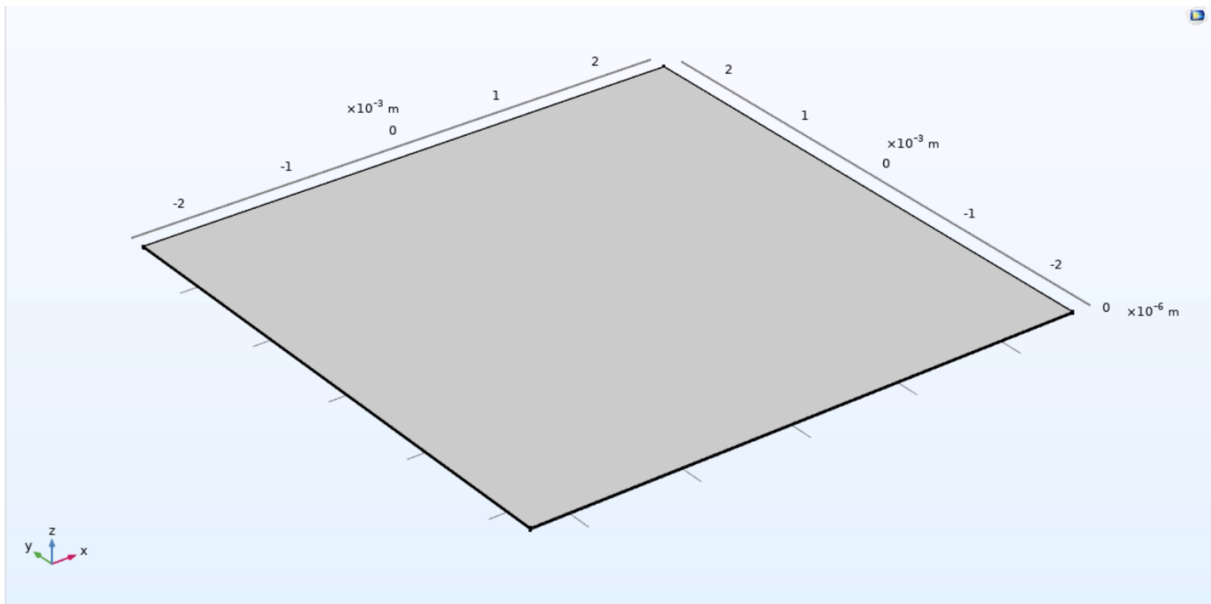


Figure 6.6: Geometry of 5x5 mm samples with two Al electrodes at top and bottom and a layer of Piezoelectric PVDF polymer in the middle as a sandwich structure in COMSOL.

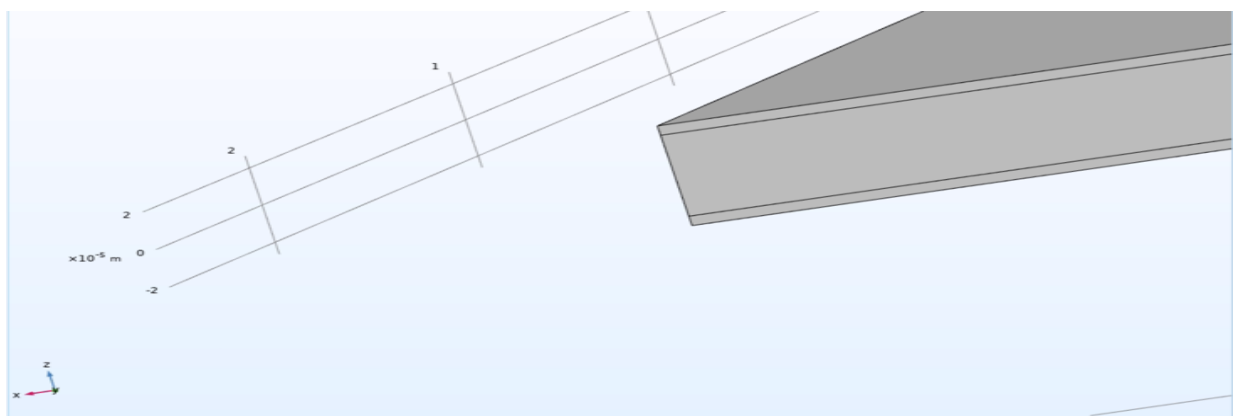


Figure 6.7 A zoomed-in photo of a sample with PVDF thickness of 43-microns and two Al electrodes at its end (one of the four samples with different PVDF thicknesses that are modeled in Comsol)

The minimum and maximum meshing sizes were set to 30 and 240 microns after checking the results of the simulations with different mesh sizes, respectively. Figure 6.8 shows the meshing size of the thin device.

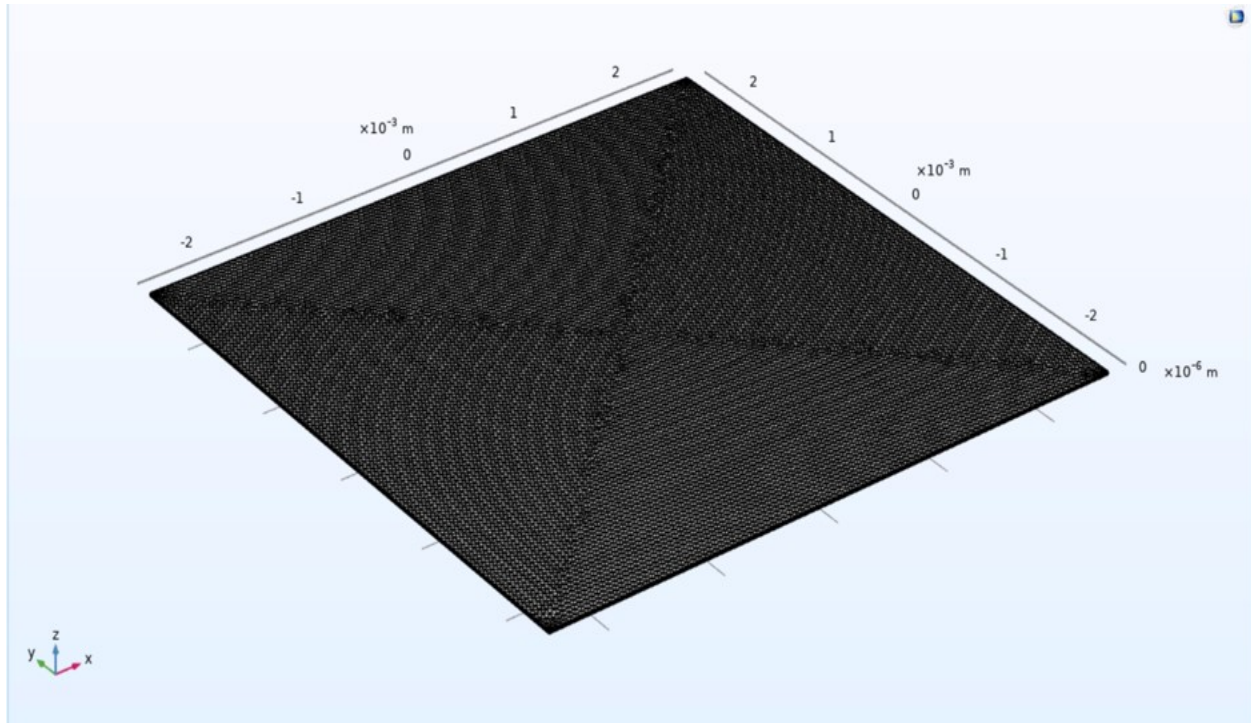


Figure 6.8 Mesh structure and fine size of the samples according to the COMSOL sizing (the mesh size of all four simulated samples is the same)

6.4.2 Force Distribution and Stress Results

In the software settings, the exact amount of the force (4.5 N) in the same direction of it (-z) is applied on the middle of the top aluminum electrode as a point load while the bottom electrode is fixed. These boundary conditions are the same for modeling four of these samples with four different thicknesses to study the effect of the thickness. Figure 6.8 illustrates the stress distribution from different points of view.

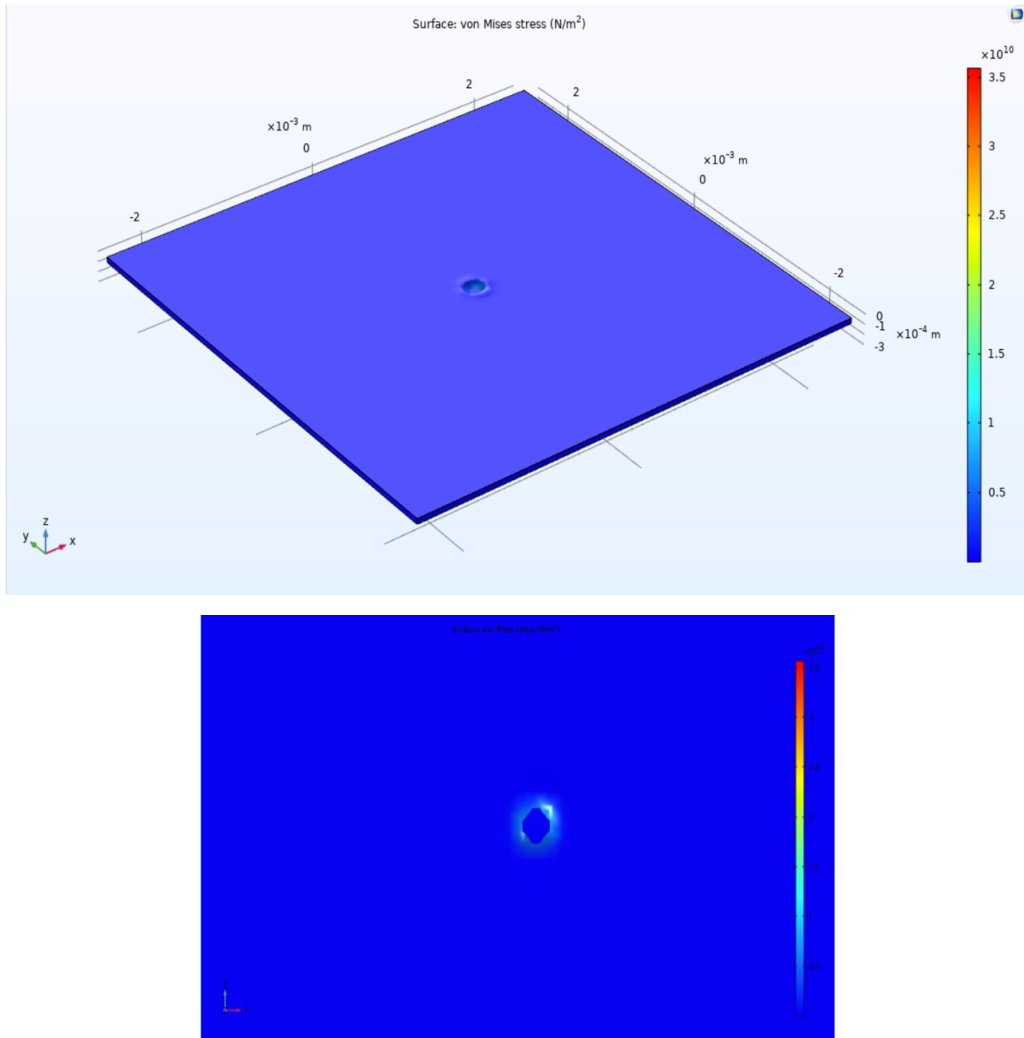


Figure 6.9 Stress results of the samples in 2D and 3D view: The load is applied in the middle of the top electrode as a point load (a point is designed on the middle of the top electrode, and then, a point load applied on that point).

6.4.3 Simulation Results and Output Voltages

The effect of the piezoelectric film thickness on the output of the system was assessed using thin polymer layers in the aforementioned configuration with thicknesses of 10, 16, 32 and 43 microns. To this end, the potential differences between the two top and bottom electrodes were investigated for each sample, and the output voltages were recorded. In figure 6.10, the performances of all the samples are illustrated.

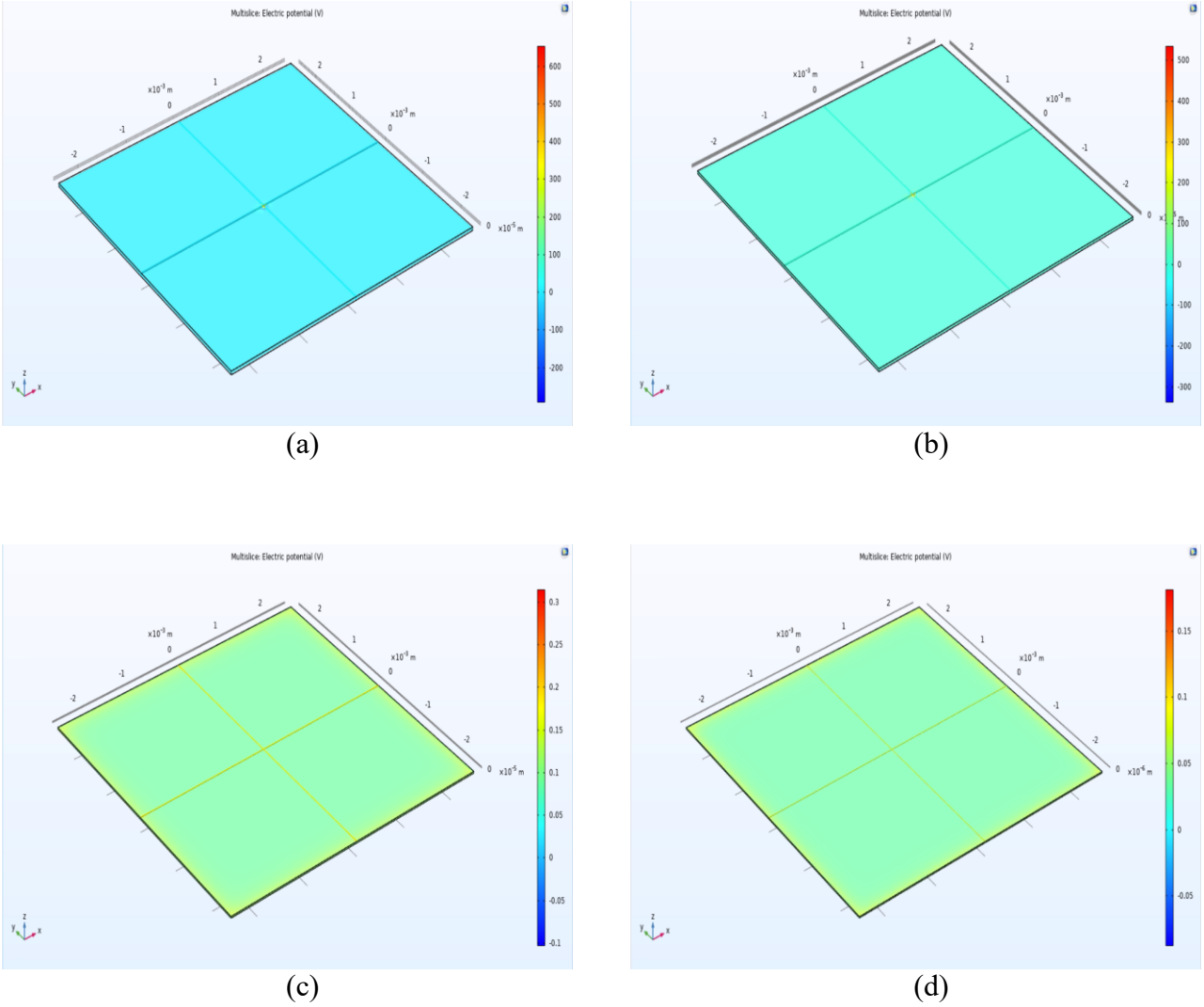


Figure 6.10 The distribution of electric potential between electrodes of the samples and the amount of the potential difference is: (a) 699 mV for PVDF layer thickness of 43 microns, (b) 491 mV for PVDF layer thickness of 32 microns, (c) 179 mV for PVDF layer thickness of 16 microns, (d) 69 mV for PVDF layer thickness of 10 microns.

6.4.4 Analysis and Comparison

As shown in figure 6.11, it can be concluded that samples with higher thicknesses in this study show better outcomes and higher generated output voltage according to the COMSOL simulations. Figure 6.11 proves that the thickness decrement of the piezoelectric material leads to a decrease in the performance of the system (lower output voltage) when the different annealing temperatures

are responsible for the cause of thickness fluctuation. Furthermore, these results confirm the effect of annealing temperature on the sample's output voltage and β phase content according to the experimental fabrication procedures. It means that the trend of voltage variation versus the sample's thickness is the same in both computer simulation and experimental approaches. The minor source of error in this comparison is due to the old experimental device and different signal noises inside the lab, which can affect the experimental results. Another reason is the presence of PVDF copolymer, TrFE, in the experimental fabrication procedure, while in the computer simulation, there is just piezoelectric PVDF in the material selection.

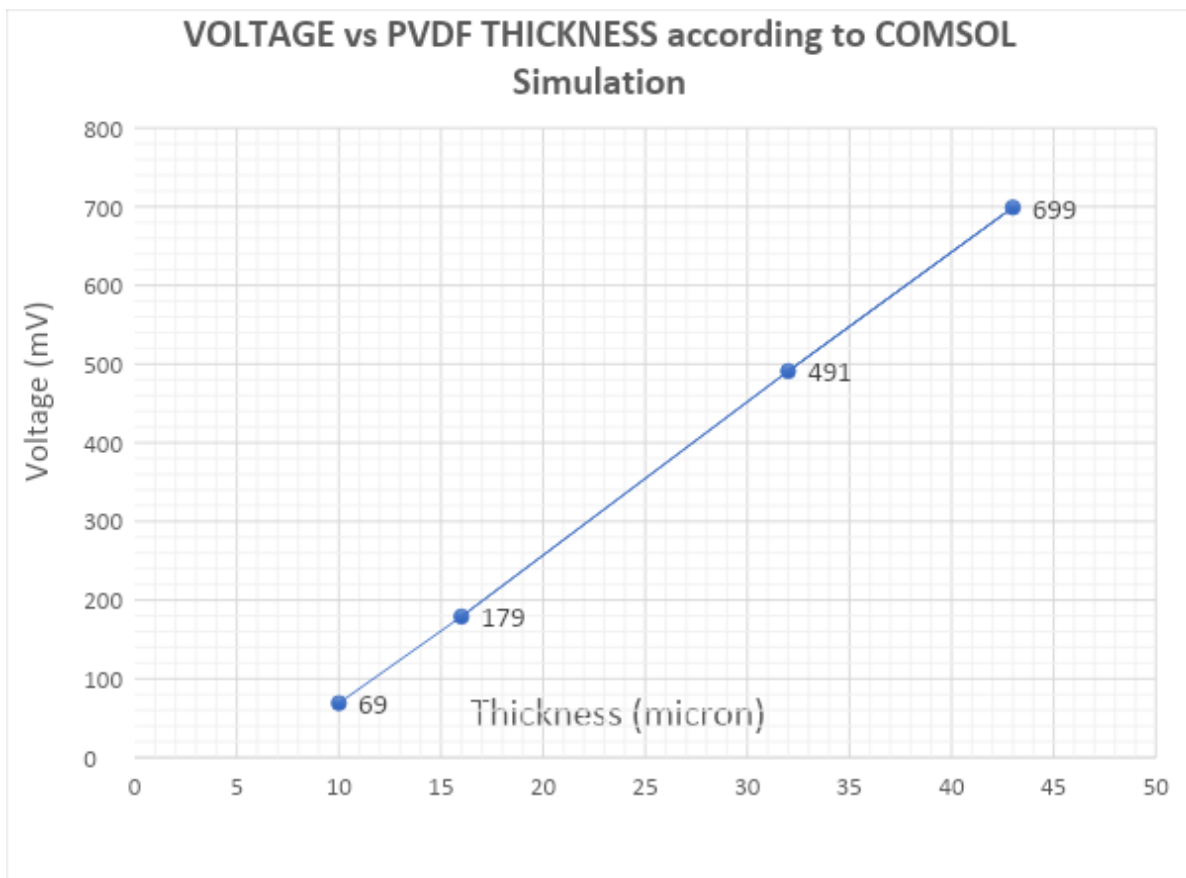


Figure 6.12 Relation between PVDF Thickness and output voltage of the samples

Chapter 7

Conclusion and Future Works

7.1 Conclusion and Contributions

In this research work, fabrication, characterization and modelling of piezoelectric PVDF-TrFE polymer as a sensor using spin-coating method was studied. To this end, the effect of various fabrication parameters on the final morphology and piezoelectric properties of PVDF-TrFE films were investigated.

To fabricate the polymer, 10% w/v PVDF-TrFE precursor solutions were produced by dissolving PVDF-TrFE powder in a mixed solvent of DMF and acetone in 50:50 volume. The solution was mixed using a magnetic stirrer, and the spin coating technique was used to coat the solution on a silicon substrate. The effect of spin-coating speed (5000 and 6000 rpm), the number of coating steps (one-step and two-steps), and post thermal annealing temperature (30, 50, and 70°C) on the final structure (in term of amount of porosities and thickness of the coating) and piezoelectric properties of PVDF-TrFE polymer films (in term of the formation of β -phase) were studied.

The obtained results showed that post thermal annealing could have a significant effect on removing the porosities from the polymer. Moreover, it was observed that increasing the annealing temperature results in producing a finer structure with less porosity. However, the FTIR results showed that increasing the annealing temperature reduces the amount of β -phase in the polymer. Moreover, it was observed that increasing the spin coating speed during the fabrication process results in higher amounts of β -phase. This can be due to the lower produced thicknesses due to the increase in the rotation speed. In the previous studies, it was shown that lower thicknesses could

improve the piezoelectric properties of PVDF. Regarding the effect of the number of coating steps, it was observed that the polymers fabricated in a single-step process were contained higher amounts of β -phase comparing to those fabricated in the double-step coating process. This can be the result of increasing the thickness of the polymer film during the double-step fabrication process.

Finally, by comparing the output voltage signal from its final testing by the Bose machine and analyzing the data, it was concluded that the produced electrical voltages due to mechanical load have direct mathematical relation with this experiment fabrication factors. Furthermore, those samples with higher β -phase content produce higher voltage and are considered to have higher piezoelectricity (figure 7.1). In the end, a computer software simulation, Comsol Multiphysics V5.5, is deployed to simulate some samples of the experiment and analyze the effect of thickness on the output voltage. The software also confirms the effect of fabrication factors on experimental results and shows the same trend as expected. As illustrated in figure 7.2, Samples with higher thicknesses due to lower thermal annealing temperatures can produce stronger signals in terms of magnitude. The reason for this phenomenon is that annealing with higher temperatures causes many transformations of β -phase into α -phase and, consequently, decreases the amount of β -phase in the polymer.

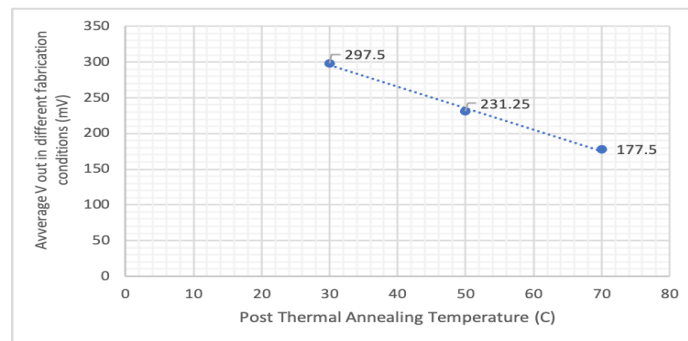


Figure 7.1 Effect of thermal annealing on average output voltage in experimental test

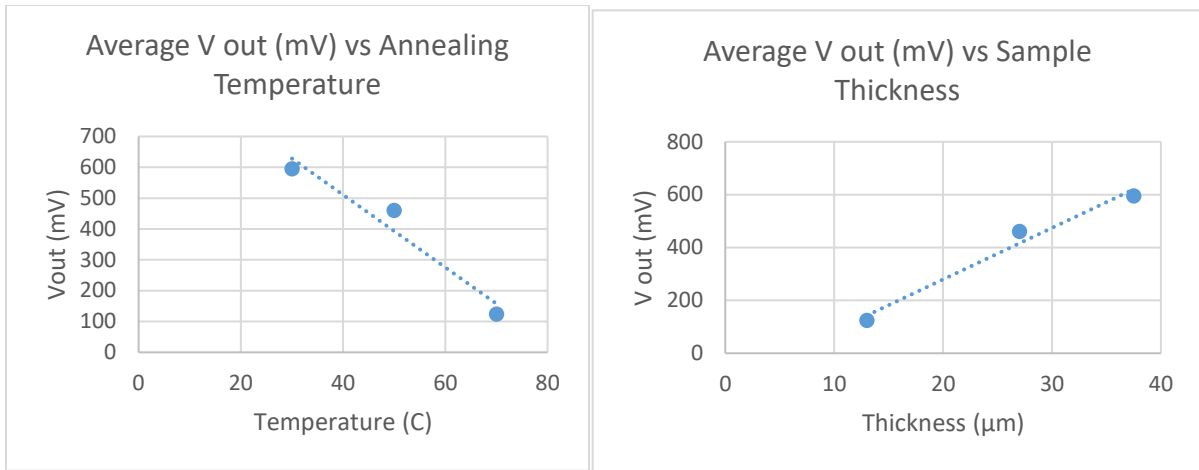


Figure 7.2 Effect of various fabrication factors on average V out according to the simulation

7.2 Future Works

7.2.1 Poling

In noncrystalline or semicrystalline synthetic polymers, it is important to pole the polymer to induce some anisotropy in the structure of the material; however, in this study, sample sensors were undergone a mechanical poling by the stretch of spin-coating process. Polling the sample will result in increasing dipole moments in the piezoelectric polymer and subsequently, will develop the polymer piezoelectric effect. Consequently, it will increase the piezoelectric strain constant resulting in higher output voltage for a given applied force.

7.2.2 Pyroelectricity Test

As it was mentioned in chapter 2, PVDF polymer has pyroelectricity properties along with its piezoelectric effect. In order to use these kinds of polymers in a specific application, it is better to have a complete understanding of their electromechanical and electrothermal properties. After identifying the electromechanical (piezoelectricity) properties of this study, electrothermal effects (pyroelectricity) should be investigated in order to know the behavior of the sensor samples and use them in a proper way for specific applications. Electrical charges will be produced by exposing the samples to a change in heat source and changing its power.

References

- [1] K. Uchino, *MicroMechatronics, Second Edition*. CRC Press, 2019.
- [2] “Ceramic Piezoelectrics - Springs and Loudspeakers,” *AZoM.com*, Feb. 21, 2001. <https://www.azom.com/article.aspx?ArticleID=95> (accessed Apr. 04, 2020).
- [3] D. Pereira, V. N. Shankar, S. Sathiyarayanan, C. Lakshmana Rao, and S. M. Sivakumar, “Vibration control of a cantilever beam using distributed PVDF actuator,” Bangalore, India, Oct. 2003, p. 598, doi: 10.1117/12.514657.
- [4] S. Hurlebaus and L. Gaul, “Smart Layer for Damage Diagnostics,” *J. Intell. Mater. Syst. Struct.*, vol. 15, no. 9–10, pp. 729–736, Sep. 2004, doi: 10.1177/1045389X04041937.
- [5] S. B. Lang and S. Muensit, “Lesser-known piezoelectric and pyroelectric applications of electroactive polymers,” *MRS Proc.*, vol. 889, pp. 0889-W01-01, 2005, doi: 10.1557/PROC-0889-W01-01.
- [6] M. A. Qasaimeh, S. Sokhanvar, J. Dargahi, and M. Kahrizi, “PVDF-based microfabricated tactile sensor for minimally invasive surgery,” *J. Microelectromechanical Syst.*, vol. 18, no. 1, pp. 195–207, 2008.
- [7] J. Dargahi, M. Kahrizi, R. N. Purushotham, and S. Sokhanvar, “Design and microfabrication of a hybrid piezoelectric-capacitive tactile sensor,” *Sens. Rev.*, vol. 26, no. 3, pp. 186–192, Jan. 2006, doi: 10.1108/02602280610675465.
- [8] J. G. Webster, *Tactile sensors for robotics and medicine*. John Wiley & Sons, Inc., 1988.
- [9] S. Najarian, J. Dargahi, and A. A. Mehrizi, *Artificial tactile sensing in biomedical engineering*. McGraw Hill Professional, 2009.
- [10] R. G. Kepler and R. A. Anderson, “Piezoelectricity and pyroelectricity in polyvinylidene fluoride,” *J. Appl. Phys.*, vol. 49, no. 8, pp. 4490–4494, Aug. 1978, doi: 10.1063/1.325454.
- [11] H. Dvey-Aharon and P. L. Taylor, “Thermodynamics of pyroelectricity and piezoelectricity in polymers,” *Ferroelectrics*, vol. 33, no. 1, pp. 103–110, Jun. 1981, doi: 10.1080/00150198108008075.
- [12] P. Ueberschlag, “PVDF piezoelectric polymer,” *Sens. Rev.*, vol. 21, no. 2, pp. 118–126, Jun. 2001, doi: 10.1108/02602280110388315.
- [13] S. B. Lang, “Pyroelectricity: From Ancient Curiosity to Modern Imaging Tool,” *Phys. Today*, vol. 58, no. 8, pp. 31–36, Aug. 2005, doi: 10.1063/1.2062916.
- [14] S. B. Lang and S. Muensit, “Review of some lesser-known applications of piezoelectric and pyroelectric polymers,” *Appl. Phys. A*, vol. 85, no. 2, pp. 125–134, Nov. 2006, doi: 10.1007/s00339-006-3688-8.

- [15] H. Kawai, “The Piezoelectricity of Poly (vinylidene Fluoride),” *Jpn. J. Appl. Phys.*, vol. 8, no. 7, pp. 975–976, Jul. 1969, doi: 10.1143/JJAP.8.975.
- [16] J. G. Bergman, J. H. McFee, and G. R. Crane, “PYROELECTRICITY AND OPTICAL SECOND HARMONIC GENERATION IN POLYVINYLIDENE FLUORIDE FILMS,” *Appl. Phys. Lett.*, vol. 18, no. 5, pp. 203–205, Mar. 1971, doi: 10.1063/1.1653624.
- [17] K. Nakamura and Y. Wada, “Piezoelectricity, pyroelectricity, and the electrostriction constant of poly(vinylidene fluoride),” *J. Polym. Sci. Part -2 Polym. Phys.*, vol. 9, no. 1, pp. 161–173, Jan. 1971, doi: 10.1002/pol.1971.160090111.
- [18] F. Mammeri, “Nanostructured flexible PVDF and fluoropolymer-based hybrid films,” in *Frontiers of Nanoscience*, vol. 14, Elsevier, 2019, pp. 67–101.
- [19] J. Nunes-Pereira, V. Sencadas, V. Correia, J. G. Rocha, and S. Lanceros-Méndez, “Energy harvesting performance of piezoelectric electrospun polymer fibers and polymer/ceramic composites,” *Sens. Actuators Phys.*, vol. 196, pp. 55–62, Jul. 2013, doi: 10.1016/j.sna.2013.03.023.
- [20] D. Gallego, N. J. Ferrell, and D. J. Hansford, “Fabrication of Piezoelectric Polyvinylidene Fluoride (PVDF) Microstructures by Soft Lithography for Tissue Engineering and Cell Biology Applications,” *MRS Proc.*, vol. 1002, pp. 1002-N04-05, 2007, doi: 10.1557/PROC-1002-N04-05.
- [21] J. Valasek, “Dielectric Anomalies in Rochelle Salt Crystals,” *Phys. Rev.*, vol. 24, no. 5, pp. 560–568, Nov. 1924, doi: 10.1103/PhysRev.24.560.
- [22] K. C. Kao, “Ferroelectrics, Piezoelectrics, and Pyroelectrics,” in *Dielectric Phenomena in Solids*, Elsevier, 2004, pp. 213–282.
- [23] B. Tandon, J. J. Blaker, and S. H. Cartmell, “Piezoelectric materials as stimulatory biomedical materials and scaffolds for bone repair,” *Acta Biomater.*, vol. 73, pp. 1–20, Jun. 2018, doi: 10.1016/j.actbio.2018.04.026.
- [24] J. Tichý, J. Erhart, E. Kittinger, and J. Přívratská, *Fundamentals of Piezoelectric Sensorics*. Berlin, Heidelberg: Springer Berlin Heidelberg, 2010.
- [25] R. Dahiya, “Piezoelectric Tactile Sensors,” in *Wiley Encyclopedia of Electrical and Electronics Engineering*, Hoboken, NJ, USA: John Wiley & Sons, Inc., 2015, pp. 1–15.
- [26] H.-P. Kim *et al.*, “Piezoelectrics,” in *Advanced Ceramics for Energy Conversion and Storage*, Elsevier, 2020, pp. 157–206.
- [27] J. Tichý and G. Gautschi, *Piezelektrische messtechnik*. Springer-Verlag Berlin, Heidelberg, New York, 1980.
- [28] J. C. Brice, “Crystals for quartz resonators,” *Rev. Mod. Phys.*, vol. 57, no. 1, pp. 105–146, Jan. 1985, doi: 10.1103/RevModPhys.57.105.
- [29] J. Detaint, J. Schwartzel, A. Zarka, B. Capelle, J. P. Denis, and E. Philippot, “Bulk wave propagation and energy trapping in the new thermally compensated materials with trigonal

symmetry,” in *Proceedings of IEEE 48th Annual Symposium on Frequency Control*, Boston, MA, USA, 1994, pp. 58–71, doi: 10.1109/FREQ.1994.398354.

[30] A. S. Bhalla, R. Guo, and R. Roy, “The perovskite structure—a review of its role in ceramic science and technology,” *Mater. Res. Innov.*, vol. 4, no. 1, pp. 3–26, Nov. 2000, doi: 10.1007/s100190000062.

[31] K. Uchino, *Piezoelectric Actuators and Ultrasonic Motors*. Springer Science & Business Media, 1996.

[32] K. Uchino, *Ferroelectric Devices*. CRC Press, 2009.

[33] H. S. Nalwa, *Ferroelectric Polymers: Chemistry: Physics, and Applications*. CRC Press, 1995.

[34] D. M. Enke, “Transducer for musical instruments,” US6248947B1, Jun. 19, 2001.

[35] A. J. Lovinger, “Ferroelectric Polymers,” *Science*, vol. 220, no. 4602, pp. 1115–1121, 1983.

[36] W. M. Prest and D. J. Luca, “The formation of the γ phase from the α and β polymorphs of polyvinylidene fluoride,” *J. Appl. Phys.*, vol. 49, no. 10, pp. 5042–5047, Oct. 1978, doi: 10.1063/1.324439.

[37] L. Ruan, X. Yao, Y. Chang, L. Zhou, G. Qin, and X. Zhang, “Properties and Applications of the β Phase Poly(vinylidene fluoride),” *Polymers*, vol. 10, no. 3, Art. no. 3, Mar. 2018, doi: 10.3390/polym10030228.

[38] R. Song, D. Yang, and L. He, “Effect of surface modification of nanosilica on crystallization, thermal and mechanical properties of poly(vinylidene fluoride),” *J. Mater. Sci.*, vol. 42, no. 20, pp. 8408–8417, Aug. 2007, doi: 10.1007/s10853-007-1787-3.

[39] A. J. Lovinger, “Conformational defects and associated molecular motions in crystalline poly(vinylidene fluoride),” *J. Appl. Phys.*, vol. 52, no. 10, pp. 5934–5938, Oct. 1981, doi: 10.1063/1.328522.

[40] Q. Zhu, V. Sharma, A. R. Oganov, and R. Ramprasad, “Predicting polymeric crystal structures by evolutionary algorithms,” *J. Chem. Phys.*, vol. 141, no. 15, p. 154102, Oct. 2014, doi: 10.1063/1.4897337.

[41] T. Furukawa, “Ferroelectric properties of vinylidene fluoride copolymers,” *Phase Transit.*, vol. 18, no. 3–4, pp. 143–211, Aug. 1989, doi: 10.1080/01411598908206863.

[42] A. J. Lovinger, “Poly(Vinylidene Fluoride),” in *Developments in Crystalline Polymers—1*, D. C. Bassett, Ed. Dordrecht: Springer Netherlands, 1982, pp. 195–273.

[43] P. Martins *et al.*, “Local variation of the dielectric properties of poly(vinylidene fluoride) during the α - to β -phase transformation,” *Phys. Lett. A*, vol. 373, no. 2, pp. 177–180, Jan. 2009, doi: 10.1016/j.physleta.2008.11.026.

- [44] J. Gomes, J. Serrado Nunes, V. Sencadas, and S. Lanceros-Mendez, "Influence of the β -phase content and degree of crystallinity on the piezo- and ferroelectric properties of poly(vinylidene fluoride)," *Smart Mater. Struct.*, vol. 19, no. 6, p. 065010, Jun. 2010, doi: 10.1088/0964-1726/19/6/065010.
- [45] H. Xu, "Dielectric properties and ferroelectric behavior of poly(vinylidene fluoride-trifluoroethylene) 50/50 copolymer ultrathin films," *J. Appl. Polym. Sci.*, vol. 80, no. 12, pp. 2259–2266, Jun. 2001, doi: 10.1002/app.1330.
- [46] P. Martins, A. C. Lopes, and S. Lanceros-Mendez, "Electroactive phases of poly(vinylidene fluoride): Determination, processing and applications," *Prog. Polym. Sci.*, vol. 39, no. 4, pp. 683–706, Apr. 2014, doi: 10.1016/j.progpolymsci.2013.07.006.
- [47] J. L. Lutkenhaus, K. McEnnis, A. Serghei, and T. P. Russell, "Confinement Effects on Crystallization and Curie Transitions of Poly(vinylidene fluoride- *co* -trifluoroethylene)," *Macromolecules*, vol. 43, no. 8, pp. 3844–3850, Apr. 2010, doi: 10.1021/ma100166a.
- [48] M. Aldas, G. Boiteux, G. Seytre, and Z. Ghallabi, "Dielectric behaviour of BaTiO₃ / P (VDF-HFP) composite thin films prepared by solvent evaporation method," in *2010 10th IEEE International Conference on Solid Dielectrics*, Potsdam, Germany, Jul. 2010, pp. 1–4, doi: 10.1109/ICSD.2010.5568042.
- [49] C. Wan and C. R. Bowen, "Multiscale-structuring of polyvinylidene fluoride for energy harvesting: the impact of molecular-, micro- and macro-structure," *J. Mater. Chem. A*, vol. 5, no. 7, pp. 3091–3128, 2017, doi: 10.1039/C6TA09590A.
- [50] Y. Huan, Y. Liu, and Y. Yang, "Simultaneous stretching and static electric field poling of poly(vinylidene fluoride-hexafluoropropylene) copolymer films," *Polym. Eng. Sci.*, vol. 47, no. 10, pp. 1630–1633, Oct. 2007, doi: 10.1002/pen.20843.
- [51] B. Ameduri, "From Vinylidene Fluoride (VDF) to the Applications of VDF-Containing Polymers and Copolymers: Recent Developments and Future Trends [†]," *Chem. Rev.*, vol. 109, no. 12, pp. 6632–6686, Dec. 2009, doi: 10.1021/cr800187m.
- [52] Z. Li, Y. Wang, and Z.-Y. Cheng, "Electromechanical properties of poly(vinylidene-fluoride-chlorotrifluoroethylene) copolymer," *Appl. Phys. Lett.*, vol. 88, no. 6, p. 062904, Feb. 2006, doi: 10.1063/1.2170425.
- [53] M. Lallart, P.-J. Cottinet, L. Lebrun, B. Guiffard, and D. Guyomar, "Evaluation of energy harvesting performance of electrostrictive polymer and carbon-filled terpolymer composites," *J. Appl. Phys.*, vol. 108, no. 3, p. 034901, Aug. 2010, doi: 10.1063/1.3456084.
- [54] K. Wongtimnoi, B. Guiffard, A. Bogner-Van de Moortèle, L. Seveyrat, C. Gauthier, and J.-Y. Cavaille, "Improvement of electrostrictive properties of a polyether-based polyurethane elastomer filled with conductive carbon black," *Compos. Sci. Technol.*, vol. 71, no. 6, pp. 885–892, Apr. 2011, doi: 10.1016/j.compscitech.2011.02.003.

- [55] J. A. Malmonge, L. F. Malmonge, G. C. Fuzari, S. M. Malmonge, and W. K. Sakamoto, "Piezo and dielectric properties of PHB-PZT composite," *Polym. Compos.*, vol. 30, no. 9, pp. 1333–1337, Sep. 2009, doi: 10.1002/pc.20719.
- [56] E. Fukada and Y. Ando, "Piezoelectric properties of poly- β -hydroxybutyrate and copolymers of β -hydroxybutyrate and β -hydroxyvalerate," *Int. J. Biol. Macromol.*, vol. 8, no. 6, pp. 361–366, Dec. 1986, doi: 10.1016/0141-8130(86)90056-5.
- [57] C. R. Bowen, H. A. Kim, P. M. Weaver, and S. Dunn, "Piezoelectric and ferroelectric materials and structures for energy harvesting applications," *Energy Env. Sci.*, vol. 7, no. 1, pp. 25–44, 2014, doi: 10.1039/C3EE42454E.
- [58] T. R. Shrout and S. J. Zhang, "Lead-free piezoelectric ceramics: Alternatives for PZT?," *J. Electroceramics*, vol. 19, no. 1, pp. 113–126, Oct. 2007, doi: 10.1007/s10832-007-9047-0.
- [59] D. Berlincourt and H. Jaffe, "Elastic and Piezoelectric Coefficients of Single-Crystal Barium Titanate," *Phys. Rev.*, vol. 111, no. 1, pp. 143–148, Jul. 1958, doi: 10.1103/PhysRev.111.143.
- [60] Y.-J. Yu and A. J. H. McGaughey, "Energy barriers for dipole moment flipping in PVDF-related ferroelectric polymers," *J. Chem. Phys.*, vol. 144, no. 1, p. 014901, Jan. 2016, doi: 10.1063/1.4939152.
- [61] F. Bauer, "Relaxor fluorinated polymers: novel applications and recent developments," *IEEE Trans. Dielectr. Electr. Insul.*, vol. 17, no. 4, pp. 1106–1112, 2010.
- [62] F. Oliveira *et al.*, "Process influences on the structure, piezoelectric, and gas-barrier properties of PVDF-TrFE copolymer," *J. Polym. Sci. Part B Polym. Phys.*, vol. 52, no. 7, pp. 496–506, 2014.
- [63] Z. Hu, M. Tian, B. Nysten, and A. M. Jonas, "Regular arrays of highly ordered ferroelectric polymer nanostructures for non-volatile low-voltage memories," *Nat. Mater.*, vol. 8, no. 1, pp. 62–67, Jan. 2009, doi: 10.1038/nmat2339.
- [64] A. Aliane, M. Benwadih, B. Bouthinon, R. Coppard, F. Domingues-Dos Santos, and A. Daami, "Impact of crystallization on ferro-, piezo- and pyro-electric characteristics in thin film P(VDF-TrFE)," *Org. Electron.*, vol. 25, pp. 92–98, Oct. 2015, doi: 10.1016/j.orgel.2015.06.007.
- [65] A. J. Lovinger, T. Furukawa, G. T. Davis, and M. G. Broadhurst, "Crystallographic changes characterizing the Curie transition in three ferroelectric copolymers of vinylidene fluoride and trifluoroethylene: 1. As-crystallized samples," *Polymer*, vol. 24, no. 10, pp. 1225–1232, Oct. 1983, doi: 10.1016/0032-3861(83)90050-2.
- [66] M. Benz, W. B. Euler, and O. J. Gregory, "The Role of Solution Phase Water on the Deposition of Thin Films of Poly(vinylidene fluoride)," *Macromolecules*, vol. 35, no. 7, pp. 2682–2688, Mar. 2002, doi: 10.1021/ma011744f.
- [67] V. F. Cardoso, G. Minas, C. M. Costa, C. J. Tavares, and S. Lanceros-Mendez, "Micro and nanofilms of poly (vinylidene fluoride) with controlled thickness, morphology and electroactive

crystalline phase for sensor and actuator applications,” *Smart Mater. Struct.*, vol. 20, no. 8, p. 087002, 2011.

[68] X. He and K. Yao, “Crystallization mechanism and piezoelectric properties of solution-derived ferroelectric poly(vinylidene fluoride) thin films,” *Appl. Phys. Lett.*, vol. 89, no. 11, p. 112909, Sep. 2006, doi: 10.1063/1.2352799.

[69] V. F. Cardoso, G. Minas, and S. Lanceros-Méndez, “Multilayer spin-coating deposition of poly(vinylidene fluoride) films for controlling thickness and piezoelectric response,” *Sens. Actuators Phys.*, vol. 192, pp. 76–80, Apr. 2013, doi: 10.1016/j.sna.2012.12.019.

[70] K. Kumar, “Microfabrication and characterization of PVDF copolymer thin films suitable for integrating with ...,” p. 159.

[71] M. Lallart, *Ferroelectrics: Physical Effects*. BoD – Books on Demand, 2011.

[72] V. Sencadas, R. Gregorio, and S. Lanceros-Méndez, “ α to β Phase Transformation and Microstructural Changes of PVDF Films Induced by Uniaxial Stretch,” *J. Macromol. Sci. Part B*, vol. 48, no. 3, pp. 514–525, May 2009, doi: 10.1080/00222340902837527.

[73] A. R. Barnett, S. M. Peelamedu, R. V. Dukkipati, and N. G. Naganathan, “Finite element approach to model and analyze piezoelectric actuators,” *JSME Int. J. Ser. C Mech. Syst. Mach. Elem. Manuf.*, vol. 44, no. 2, pp. 476–485, 2001.

[74] H. F. Tiersten, “Coupled magnetomechanical equations for magnetically saturated insulators,” *J. Math. Phys.*, vol. 5, no. 9, pp. 1298–1318, 1964.